

RECEIVED: April 4, 2022 REVISED: July 18, 2022 ACCEPTED: August 5, 2022 PUBLISHED: August 30, 2022

# Sensitivity to dark sector scales from gravitational wave signatures

James B. Dent, a Bhaskar Dutta, b Sumit Ghosh, b,c Jason Kumar and Jack Runburg d

<sup>a</sup> Department of Physics, Sam Houston State University, Huntsville, TX 77341, U.S.A.

<sup>b</sup> Mitchell Institute for Fundamental Physics and Astronomy, Department of Physics and Astronomy, Texas A&M University, College Station, Texas 77843, U.S.A.

<sup>c</sup>School of Physics, Korea Institute for Advanced Study, Seoul 02455, Korea

<sup>d</sup>Department of Physics and Astronomy, University of Hawaii, Honolulu, Hawaii 96822, U.S.A.

E-mail: jbdent@shsu.edu, dutta@physics.tamu.edu, ghosh@kias.re.kr, jkumar@hawaii.edu, runburg@hawaii.edu

ABSTRACT: We consider gravitational sound wave signals produced by a first-order phase transition in a theory with a generic renormalizable thermal effective potential of power law form. We find the frequency and amplitude of the gravitational wave signal can be related in a straightforward manner to the parameters of the thermal effective potential. This leads to a general conclusion; if the mass of the dark Higgs is less than 1% of the dark Higgs vacuum expectation value, then the gravitational wave signal will be unobservable at all upcoming and planned gravitational wave observatories. Although the understanding of gravitational wave production at cosmological phase transitions is still evolving, we expect this result to be robust.

KEYWORDS: Early Universe Particle Physics, Phase Transitions in the Early Universe, Cosmology of Theories BSM

ArXiv ePrint: 2203.11736

$\mathbf{C}$	ontents			
1	Introduction	1		
2	First-order phase transitions with a renormalizable scalar potential 2.1 Thermal parameters of the phase transition 2.2 The gravitational wave signal	<b>2</b> 4 5		
3	Results	7		
4	4 Conclusions			

#### 1 Introduction

With the advent of gravitational wave (GW) detection [1], and the development of new instruments (see table 1, and references therein), gravitational wave signals have become among the most promising signatures for new physics beyond the Standard Model (SM) in the early Universe. In particular, cosmological first order phase transitions in the early Universe can generate gravitational wave signatures [2–6] which can be observed at current and upcoming experiments (for reviews, see [7–13]). Considerable work has focused on determining if particular models can produce GW signals which are observable at upcoming experiments. There has been a recent flurry of works examining extensions of the Standard Model which could provide gravitational wave signatures [14–63], including models with a focus on dark sectors and dark matter [64–100].

In this work, we approach this problem from a different angle. We scan the parameter space of a simple and well-motivated thermal effective potential with a single dark Higgs field, which can arise from a wide class of UV-complete models. We correlate the properties of the GW signal arising from a first-order phase transition with the parameters of the effective potential (for other work examining general models, as well as model and signal features and classes, see for example, [101–110], including cosmological contraints [111], non-gaussianities [112], and circular polarization [113]).

The result of this analysis is a characterization of the sound wave GW signal which can arise from any UV-complete model whose thermal effective potential is polynomial and renormalizable. Interestingly, we find that dimensional analysis and scaling relations control much of the analysis, allowing us to relate specific features of the GW signal to specific parameters of the effective potential.

As a specific example, we find that amplitude of the gravitational wave signal is strongly related to the ratio of the dark Higgs mass to the dark Higgs vacuum expectation value (vev) at zero temperature. If the dark Higgs mass is less than  $\mathcal{O}(1\%)$  of the dark Higgs vev, then the GW signal will be too small to be observed at any upcoming experiments. Because

the amplitude of the signal scales as several powers of ratio of dark Higgs mass to vev, our result is robust. Indeed, theoretical work connecting the amplitude of a gravitational wave signal to the underlying parameters of the phase transition is constantly evolving (for example, more refined calculations for determining the kinetic energy fraction [114–116], the wall velocity [117–119], and adoption of more general parameterized forms for the frequency spectra [120] which can account for the variations from different studies, such as [121–129]), leading one to wonder how well one can trust any even state-of-the-art result. But in order to change our bound by an order-of-magnitude, one would need a correction to the gravitational wave signal of many orders of magnitude, giving our result some robustness to future developments.

We also find a general relationship between the symmetry-breaking vev and peak frequency of the GW signal. We then characterize the optimal instruments for probing generic first-order phase transitions, in terms of the symmetry-breaking scale at zero temperature.

But it is also important to point out what we do not do — we do not provide a complete analysis of any particular UV-complete model. We assume a thermal effective potential for a single scalar field which is renormalizable and of the polynomial form. Although well-motivated, for any particular model, this may or may not be a good approximation to the thermal effective potential. Our results apply directly to models for which this thermal effective potential is a good approximation, while for other models, our results are at best indicative.

The plan of this paper is as follows. In section 2, we parameterize the thermal effective potential, and characterize the allowed phase transitions and resulting gravitational wave signals. In section 3, we describe the results of our scans over the parameter space of the thermal effective potential. We conclude in section 4 with a discussion of our results.

# 2 First-order phase transitions with a renormalizable scalar potential

We consider a thermal effective potential for a single real scalar field  $\phi$ . We consider a renormalizable polynomial potential [65] of the form

$$V(T,\phi) = \Lambda^4 \left[ \left( -\frac{1}{2} + c \left( \frac{T}{v} \right)^2 \right) \left( \frac{\phi}{v} \right)^2 + b \frac{T}{v} \left( \frac{\phi}{v} \right)^3 + \frac{1}{4} \left( \frac{\phi}{v} \right)^4 \right], \tag{2.1}$$

where  $V(T=0,\phi)$  is minimized at  $\phi=\pm v$ , and where the mass of the dark Higgs (the excitation of  $\phi$  about this minimum) is given by  $m^2/v^2=2(\Lambda/v)^4$ . This form of the potential arises, for example, from thermal corrections in the high temperature limit, where the dimensionless coefficients b and c depend on the details of the UV model. We assume  $\Lambda/v \lesssim 1$ , ensuring that effective potential has a perturbative quartic coupling. We also take b < 0, as this coefficient arises in the high temperature limit from fermion loops which contribute with a negative sign to the effective potential.

It is convenient to express the potential in terms of the scale-free quantities  $\tilde{\phi} = \phi/v$  and  $\tilde{T} = T/v$ . Essentially, the symmetry-breaking scale v is used as the scale against which

all other energies are measured. Defining  $\tilde{V}(\tilde{T},\tilde{\phi})=\Lambda^{-4}V(T,\phi)$ , we have

$$\tilde{V}\left(\tilde{T},\tilde{\phi}\right) = \left(-\frac{1}{2} + c\tilde{T}^2\right)\tilde{\phi}^2 + b\tilde{T}\tilde{\phi}^3 + \frac{1}{4}\tilde{\phi}^4. \tag{2.2}$$

We can now consider the generic behavior of this thermal effective potential. At finite temperature, the potential can have up to three extrema, at  $\phi = 0$  and at factor of 2 under the radical is fixed

$$\tilde{\phi} = \frac{-3b\tilde{T} \pm \sqrt{9b^2\tilde{T}^2 + 4\left(1 - 2c\tilde{T}^2\right)}}{2}.$$
(2.3)

If  $c\tilde{T}^2 < (1/2) + (9/8)b^2\tilde{T}^2$ , then the discriminant is positive, and three distinct extrema exist. In that case, one extremum is a local maximum, while the other two are local minima, and at least one is a symmetry-breaking minimum.

 $V(T,\phi=0)=0$ , where this extremum at  $\phi=0$  is a local minimum for  $c\tilde{T}^2>1/2$  and a local maximum for  $c\tilde{T}^2<1/2$ . The condition for  $V(T,\phi)=0$  for  $\phi>0$  is

$$c\tilde{T}^2 \le \frac{1}{2} + b^2 \tilde{T}^2. \tag{2.4}$$

We can thus classify the behavior of the potential as the Universe cools from high temperature. At sufficiently high temperature, the symmetry-preserving extremum is always a local minimum at V=0. But for  $c/b^2<1$ , the potential has two other zeros, with a global minimum between them, even at high temperature. In this case, there is no phase transition, since the Universe is always in the symmetry-breaking phase. We thus restrict ourselves to the case  $c/b^2>1$ .

For  $c/b^2 > 1$ , then at high temperature there is a global minimum at  $\phi = 0$  and a local minimum at  $\phi_+ > 0$ , with a local maximum at  $\phi_-$  between them. But at low enough temperature  $(\tilde{T}_C = 1/\sqrt{2(c-b^2)})$ , we find  $V(\phi_+) = 0$ .

For  $T < T_C$ ,  $\phi_+$  is now the global minimum, and a first-order phase transition is possible. The transition will not occur until the nucleation temperature,  $T_N$ , at which time the bubble nucleation rate is larger than the Hubble expansion rate. But at sufficiently low temperature ( $\tilde{T} < 1/\sqrt{2c}$ ), the potential barrier goes to zero; the symmetry-preserving extremum is now a local maximum, and if the phase transition has not yet completed, then  $\phi$  can simply roll to the global minimum, yielding a second-order phase transition.

Note that our analysis of the minima of the potential depended only on the parameters b and c, as v appears only as a scale parameter, and  $\Lambda$  has factored out. But the dependence on  $\Lambda$  returns when we determine the nucleation temperature. The bubble nucleation rate per unit volume (p(T)) is given by  $p(T) = T^4 \exp[-S_E/T]$ , where  $S_E$  is the Euclidean action for the radial bounce solution between the symmetry-preserving and symmetry-breaking vacua. The nucleation temperature  $T_N$  is the temperature at the nucleation time  $t_N$ , at which a fraction  $e^{-1}$  of the Universe has tunnelled to the global minimum of the potential. The nucleation time is given approximately by the relation  $p(t_N)t_N^4 = 1$ . Assuming a radiation-dominated universe with  $g_* = \mathcal{O}(100)$  relativistic degrees of freedom, we then find [12, 130-132]

$$\frac{S_E}{T_N} = 140 + \mathcal{O}\left(\log T_N/\text{TeV}\right). \tag{2.5}$$

 $S_E$  is the Euclidean action evaluated on the bounce solution to the radial equation [131, 133]

$$\frac{d^2\phi}{dr^2} + \frac{2}{r}\frac{\partial\phi}{\partial r} = \frac{\partial V_E(T,\phi)}{\partial\phi}.$$
 (2.6)

where  $V_E(T, \phi)$  is the temperature and field dependent potential in the Euclidean action. This solution interpolates between  $\phi = 0$  and  $\phi = \phi_+$ . We will utilize an analytic approximation to the bounce solution for this form of the effective potential [134], given by

$$\frac{S_E}{T} = \frac{4.85M^3}{E^2T^3} \left[ 1 + \frac{\alpha}{4} \left( 1 + \frac{2.4}{1 - \alpha} + \frac{0.26}{(1 - \alpha)^2} \right) \right],\tag{2.7}$$

where

$$M^2 \equiv 2\frac{\Lambda^4}{v^2} \left( \frac{cT^2}{v^2} - \frac{1}{2} \right), \qquad E \equiv -\frac{b\Lambda^4}{v^4}, \qquad \alpha \equiv \frac{M^2\Lambda^4}{2E^2T^2v^4}.$$
 (2.8)

For certain models, this analytic solution was compared to the Euclidean action computed using CosmoTransitions [131], a Python package that numerically computes the properties of phase transitions in scalar field theories, and good agreement was found. A more detailed comparison was performed in [135], similarly finding good agreement.

To put eq. (2.6) in scale-free form, we define  $\tilde{r} \equiv r(\Lambda^2/v)$ , yielding

$$\frac{d^2\tilde{\phi}}{d\tilde{r}^2} + \frac{2}{\tilde{r}}\frac{\partial\tilde{\phi}}{\partial\tilde{r}} = \frac{\partial\tilde{V}_E\left(\tilde{T},\tilde{\phi}\right)}{\partial\tilde{\phi}}.$$
(2.9)

The scale-free Euclidean action,  $\tilde{S}_E$ , is obtained by integrating the scale-free Lagrangian, evaluated on the bounce solution of the above equation, with respect to  $d^3\tilde{r}$   $d(1/\tilde{T})$ , and is related to  $S_E$  by

$$\frac{S_E}{T} = \frac{v^2}{\Lambda^2} \frac{\tilde{S}_E}{\tilde{T}}.$$
 (2.10)

We thus find

$$\frac{\tilde{S}_E}{\tilde{T}_N} \sim 140 \left(\frac{\Lambda}{v}\right)^2,$$
 (2.11)

where the left-hand side of eq. (2.11) depends only on b, c and  $\tilde{T}_N$ .

## 2.1 Thermal parameters of the phase transition

We are now able to determine  $S_E(\tilde{T})$  and  $\tilde{T}_N$  for any parameters b, c and  $\Lambda/v$ . From these, we can determine the thermal parameters of the phase transition, which in turn feed into the gravitational wave signature. These are speed parameter of the phase transition  $(\beta/H)$ , and the latent heat parameter  $(\xi)$ .

We can write the thermal parameters as

$$\left(\frac{\beta}{H}\right) = \left(\frac{\tilde{\beta}}{H}(b, c, \Lambda/v)\right) \times \left(\frac{\Lambda}{v}\right)^{-2},$$

$$\xi = \tilde{\xi}(b, c, \Lambda/v) \times \left(\frac{\Lambda}{v}\right)^{4} \left(\frac{g_{*}}{100}\right)^{-1},$$
(2.12)

where

$$\frac{\tilde{\beta}}{H}(b,c,\Lambda/v) = \left(\tilde{T}\frac{d\left(\tilde{S}_{E}/\tilde{T}\right)}{d\tilde{T}}\right)_{\tilde{T}=\tilde{T}_{N}},$$

$$\tilde{\xi}(b,c,\Lambda/v) = \left[\left(\frac{3}{10\pi^{2}\tilde{T}_{N}^{4}}\right)\left(\Delta\tilde{V}-\tilde{T}\Delta\frac{d\tilde{V}}{d\tilde{T}}\right)\right]_{\tilde{T}=\tilde{T}_{N}},$$
(2.13)

and  $g_*$  is the number of relativistic degrees of freedom. Essentially, the parameter  $\Lambda/v$  controls an overall rescaling of the potential, and the power-law dependence of the thermal parameters on  $\Lambda/v$  in eq. (2.12) encodes the dependence of these parameters on that scaling.

Note that the scale-free thermal parameters  $(\tilde{\beta}/H)$  and  $\tilde{\xi}$  depend on  $\Lambda/v$  only through the determination of the scale-free nucleation temperature,  $\tilde{T}_N$ . Thus, the actual thermal parameters  $(\beta/H)$  and  $\xi$  have a dependence on  $\Lambda/v$  which is nearly power-law. This dependence would be exactly power law if the nucleation temperature were exactly the same as the critical temperature. In fact, the nucleation temperature will be less than the critical temperature, leading to a deviation from power-law behavior. But we will see that this power-law behavior largely determines the maximum allowed gravitational wave signal. Moreover, this form of the thermal effective potential is a good approximation in the high temperature limit; if the nucleation temperature is significantly smaller than the critical temperature, this may not be a good approximation. A typical scale where the high-temperature approximation remains valid is given by  $T \gtrsim m$  (for example, in [65] the criteria  $T^2 > 2m^2$  was employed). This can be translated to the constraint  $\tilde{T} \gtrsim \sqrt{2}(\Lambda/v)^2$ . However, the size of the effects of non-power law terms that would be generated if this criteria is not met would be model dependent, thus we do not pursue that line of inquiry further in this work.

# 2.2 The gravitational wave signal

First order phase transitions can produce gravitational waves via three different mechanisms: i) bubble collisions, ii) sound waves from bubble expansion in the fluid, and iii) turbulence in the fluid. In a runaway bubble expansion, where bubble wall velocities are not sufficiently slowed by friction from the fluid, bubble collisions can provide the dominant gravitational wave signal. This situation can arise, for example, for extremely supercooled systems [125, 136, 137]. The study of turbulence is ongoing, with the efficiency of converting kinetic energy into turbulent energy being one source of some uncertainty [109, 122, 129]. Thus, as we are not examining extremely supercooled situations, we will assume that the dominant gravitational wave signature arises from sound waves [138]. We can express the amplitude  $(h^2\Omega_{sw})$  and frequency  $(f_{sw})$  of this gravitational wave signal as [8, 135, 139]

$$h^2 \Omega_{sw}(f) = h^2 \Omega_{sw}^{\text{max}} \times \left(\frac{f}{f_{sw}}\right)^3 \left(\frac{7}{4 + 3(f/f_{sw})^2}\right)^{7/2},$$
 (2.14)

where

$$f_{sw} = \tilde{f}_{sw}(b, c, \Lambda/v) \times \left(\frac{\Lambda}{v}\right)^{-2} \left(\frac{T_N}{100 \text{ GeV}}\right) \left(\frac{g_*}{100}\right)^{1/6},$$

$$h^2 \Omega_{sw}^{\text{max}} = h^2 \tilde{\Omega}_{sw}^{\text{max}}(b, c, \Lambda/v) \times \left(\frac{\Lambda}{v}\right)^{10+8n} \left(\frac{g_*}{100}\right)^{-5/3-2n} \times \left[1 - \frac{1}{\sqrt{1 + 2\tau_{sh}H_s}}\right],$$
(2.15)

and [114]

$$\tilde{f}_{sw}(b, c, \Lambda/v) = 8.9 \times 10^{-3} \text{mHz} \left(\frac{1}{v_w}\right) \left(\frac{\tilde{\beta}}{H}\right) \left[\times \left(\frac{z_p}{10}\right) \frac{1}{\sqrt{1 + 2\tau_{sh}H_s}}\right],$$

$$h^2 \tilde{\Omega}_{sw}^{\text{max}}(b, c, \Lambda/v) = 8.5 \times 10^{-6} \left(\frac{\Gamma}{4/3}\right)^2 (\tilde{\kappa}_f \tilde{\xi})^2 \left(\frac{\tilde{\beta}}{H}\right)^{-1} v_w,$$

$$\tilde{\kappa}_f \sim \tilde{\xi}^n. \tag{2.16}$$

Here,  $v_w$  is the sound speed, which determines the exponent n; for  $v_w \sim 1$ , we have n = 1, while for  $v_w \sim 0.5$ , we have  $n \sim 2/5$  [114].  $\Gamma$  is the adiabatic index, which we will take to be  $\Gamma = 4/3$  [65], and  $z_p \sim 10$  [123, 135].

There are additional factors listed in brackets [135], which depend on the details of the model, encoded in quantities such as the time scale for turbulence  $(\tau_{sh})$  and the Hubble scale at which the source becomes active  $(H_S)$ . Indeed, as pointed out in [139], there are a variety of suppression factors which can arise from a more diligent treatment of gravitational wave production, which can suppress the signal amplitude by more than an order of magnitude. As we begin with an effective potential for the scalar, but no detailed microphysics, it is not possible to attain this level of precision. But for our purpose, it is not necessary. Since the gravitational wave amplitude scales as more than 10 powers of  $(\Lambda/v)$ , this analysis will be sufficient to determine classes of models which will be easily inaccessible to all upcoming experiments. Moreover, although future theoretical developments may uncover additional correction factors, unless their collective size is several orders of magnitude, they will not change our results appreciably. For similar reasons, it is sufficient for us define the thermal parameters at the nucleation temperature, rather than the percolation temperature.

In a similar vein, there are a variety of theoretical uncertainties with both the first-order phase transition and the associated gravitational wave signature, and there has been much recent theoretical progress, including studies of gauge dependence, renormalization group equations, and the one-loop effective potential [140, 141], discussions within an effective field theory framework [142–144], issues related to the perturbative expansion including its scale dependence [145–148], and non-perturbative models and resummation and use of numerical simulations (for example, see [115, 121–123, 125, 126, 149–155]). It would be interesting to incorporate these effects in a more detailed analysis, but it is not necessary for our purpose here.

The main quantities we are interested in are the peak amplitude of the GW signal  $(h^2\Omega_{sw}^{\max})$ , and the frequency at which that peak is obtained  $(f_{sw})$ . If the nucleation temperature were equal to the critical temperature, then  $h^2\tilde{\Omega}_{sw}^{\max}$  and  $\tilde{f}_{sw}$  would be independent of

 $\Lambda/v$ , the dependence of the GW signal parameters on  $\Lambda/v$  would be entirely determined by the scaling relations in eq. (2.12). We would then find

$$\left(h^2 \Omega_{sw}^{\text{max}}\right)_{T_N = T_C} \propto \xi^{2(n+2)} \left(\frac{\beta}{H}\right)^{-1} \propto \left(\frac{\Lambda}{v}\right)^{10+8n},$$

$$(f_{sw})_{T_N = T_C} \propto \frac{\beta}{H} v \propto \left(\frac{\Lambda}{v}\right)^{-2} v,$$
(2.17)

where  $(\Lambda/v)^4 = m^2/2v^2$ , and the power-law dependence on  $\Lambda/v$  is induced by the dependence of the thermal parameters on the overall scale of the potential.

Reducing m/v by an order of magnitude would reduce the amplitude of the GW signal by a factor of at least  $10^5$  (taking n=0). We thus expect to find a sharp minimum for m/v; for dark Higgs masses which are sufficiently smaller than the symmetry-breaking scale, the amplitude of the GW signal will be unobservable.

Note, however that although the amplitude of the GW signal depends on m/v, it has no actual dependence on v itself, a result which could be anticipated from dimensional analysis. But the symmetry-breaking scale does enter into  $f_{sw}$ , to which it is directly proportional. Thus far, our analysis has been completely scale-free. We now see that the energy scale of the phase transition only enters in the last step, setting the frequency scale of the GW signal.

Some of these considerations will be modified once we include the dependence of the nucleation temperature on  $(\Lambda/v)$ . But we expect that this modification should not change the result substantially; if  $T_N \ll T_C$ , then the phase transition is very supercooled, and this form of the thermal effective potential may in any case not be a good approximation to the thermal potential of a UV complete model. We will see from more detailed numerical calculation that this intuition is correct.

## 3 Results

In this section, we describe our strategy for scanning over the parameter space of the thermal effective potential and then present the results of the scan. First, we briefly specify the conditions for a parameter space point to be of interest.

- $\Lambda/v < 1$ : this condition ensures that the zero-temperature quartic coupling is perturbative.
- $c/b^2 > 1$ : this condition is required for a phase transition to occur at all. If it is not satisfied, then the symmetry-breaking minimum is the global minimum even at high temperature.
- $c\tilde{T}_N^2 > 1/2$ : this is necessary in order for the transition to be first-order. If this is not satisfied, then the barrier disappears before the nucleation temperature is reached, leading to a smooth phase transition.
- $\beta/H > 1$ : this condition is needed for the bubble growth rate to exceed the Hubble expansion, so that bubbles grow. This is equivalent to  $\tilde{\beta}/H > (\Lambda/v)^2$ .

•  $\xi > 0$ : a first order transition will only proceed if the latent heat parameter is positive at the nucleation temperature. This is equivalent to  $\tilde{\xi} > 0$ .

It may seem unusual that the latent heat parameter can be negative. It is easy to demonstrate that, if the phase transition occurs at the critical temperature, then the latent heat parameter must be positive. But it may become negative if the phase transition is sufficiently supercooled. As we have already mentioned, such a transition would potentially stretch the effective potential beyond its regime of validity. But in any case, if the latent heat parameter is negative, no GW signal will be produced.

The scale-free Euclidean action,  $\tilde{S}_E$ , is determined by  $\tilde{T}$  and the parameters b and c. For any choice of parameters b, c and  $\Lambda/v$ , the nucleation temperature  $\tilde{T}_N$  is approximately determined by the solution of the equation

$$\frac{\tilde{S}_E(b, c, \tilde{T}_N)}{140\tilde{T}_N} = \left(\frac{\Lambda}{v}\right)^2. \tag{3.1}$$

In figures 1 and 2, we plot contours of  $\tilde{S}_E(b, c, \tilde{T})/140\tilde{T}$  in the (b, c)-plane, for eight different choices of  $\tilde{T}$ . We can then solve eq. (3.1) by setting  $(\Lambda/v)^2$  equal to the  $\tilde{S}_E/140\tilde{T}$ , for a value of  $\tilde{T}$  which is taken as the nucleation temperature. These figures thus encode all choices of the parameters  $(b, c, \Lambda/v)$  for which the scale-free nucleation temperature is given by a particular choice  $\tilde{T}_N$ . Note, we only plot parameters points which are of interest, as defined by the criteria described at the beginning of this section.

Note that the range of parameter space which is of interest is very small for  $\tilde{T}_N \sim 1$ , near  $(b,c) \sim (-\sqrt{2},2)$ . More parameter space is available for  $\tilde{T}_N < 1$ , and for relatively large  $\tilde{T}_N$ , the available parameter space is focused near the curve  $c=b^2$ . But as  $\tilde{T}_N$  becomes small, the high temperature approximation becomes less valid; in that case, it is not clear if this effective potential can be realized from a UV complete model. In particular, note that, although we do not consider the range c>25 for reasons of computational ease, that range in any case corresponds to small  $\tilde{T}_N$ .

In figures 3 and 4, we plot contours of  $\tilde{\beta}/H$  in the (b,c)-plane, for different choices of  $\tilde{T}_N$ . Only parameter points satisfying the criteria described in the beginning of this section are considered. In particular, for any choice of  $\tilde{T}_N$ , only points in the (b,c)-plane are shown for which there exists some choice of  $\Lambda/v$  consistent with the given  $\tilde{T}_N$ .

Similarly, in figures 5 and 6, we plot contours of  $\tilde{\xi}$  in the (b,c)-plane for different choices of  $\tilde{T}_N$ . Note that unless  $\tilde{T}_N \ll 1$ , we find  $\tilde{\xi} \lesssim \mathcal{O}(10)$  throughout the entire parameter space. This implies that, unless the phase transition occurs well below the symmetry breaking scale, we will find

$$h^{2}\tilde{\Omega}_{sw}^{\max} < \mathcal{O}(0.1),$$

$$h^{2}\Omega_{sw}^{\max} < \mathcal{O}(0.1) \left(\frac{\Lambda}{v}\right)^{10+8n}$$
(3.2)

The maximum sensitivity of LISA is roughly  $h^2\tilde{\Omega}_{sw} \sim \mathcal{O}(10^{-13})$ , implying that LISA will be insensitive to any model for which  $\Lambda/v \lesssim \mathcal{O}(10^{-1})$ . Note that we can directly relate the parameters of the thermal effective potential to the mass and vev of the dark Higgs at

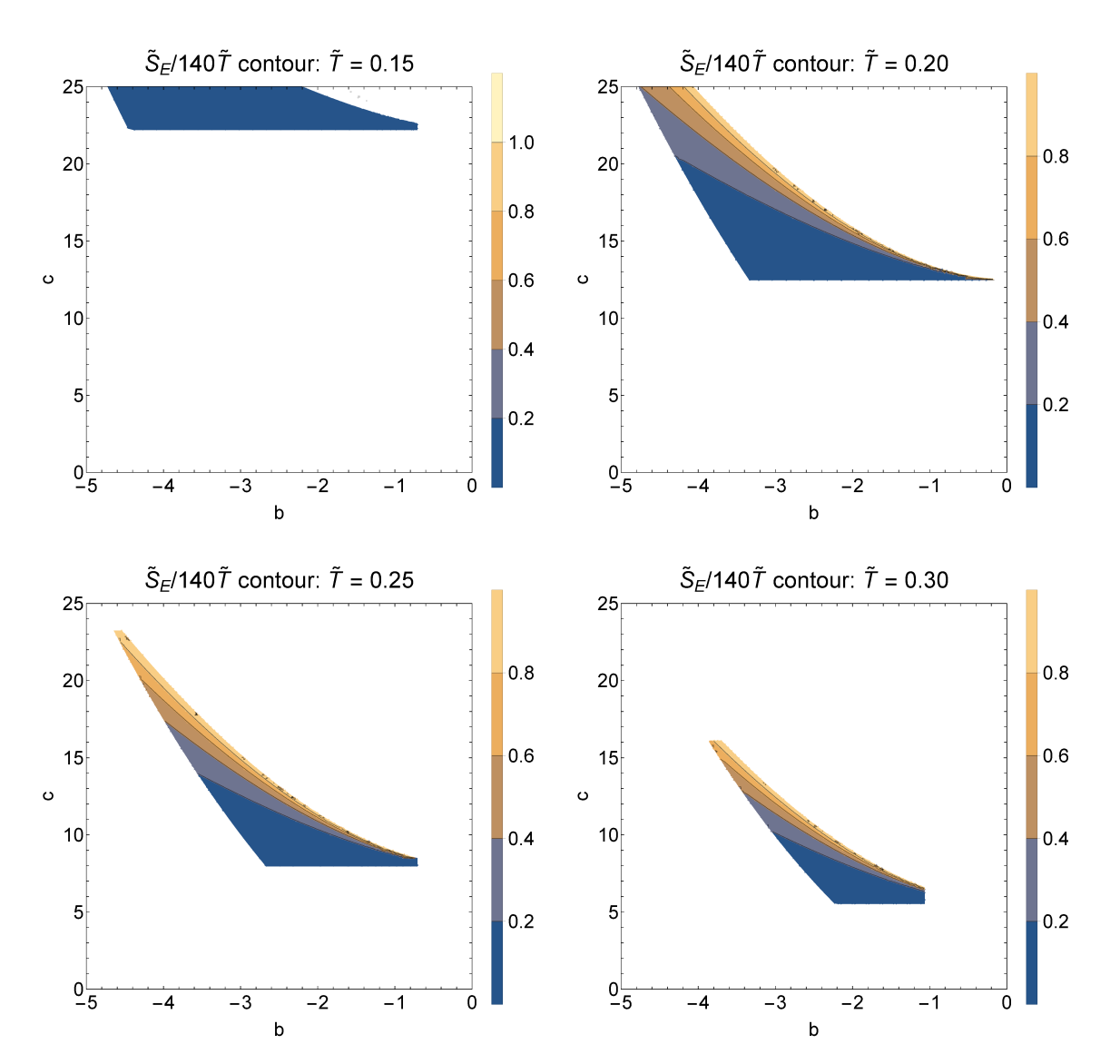
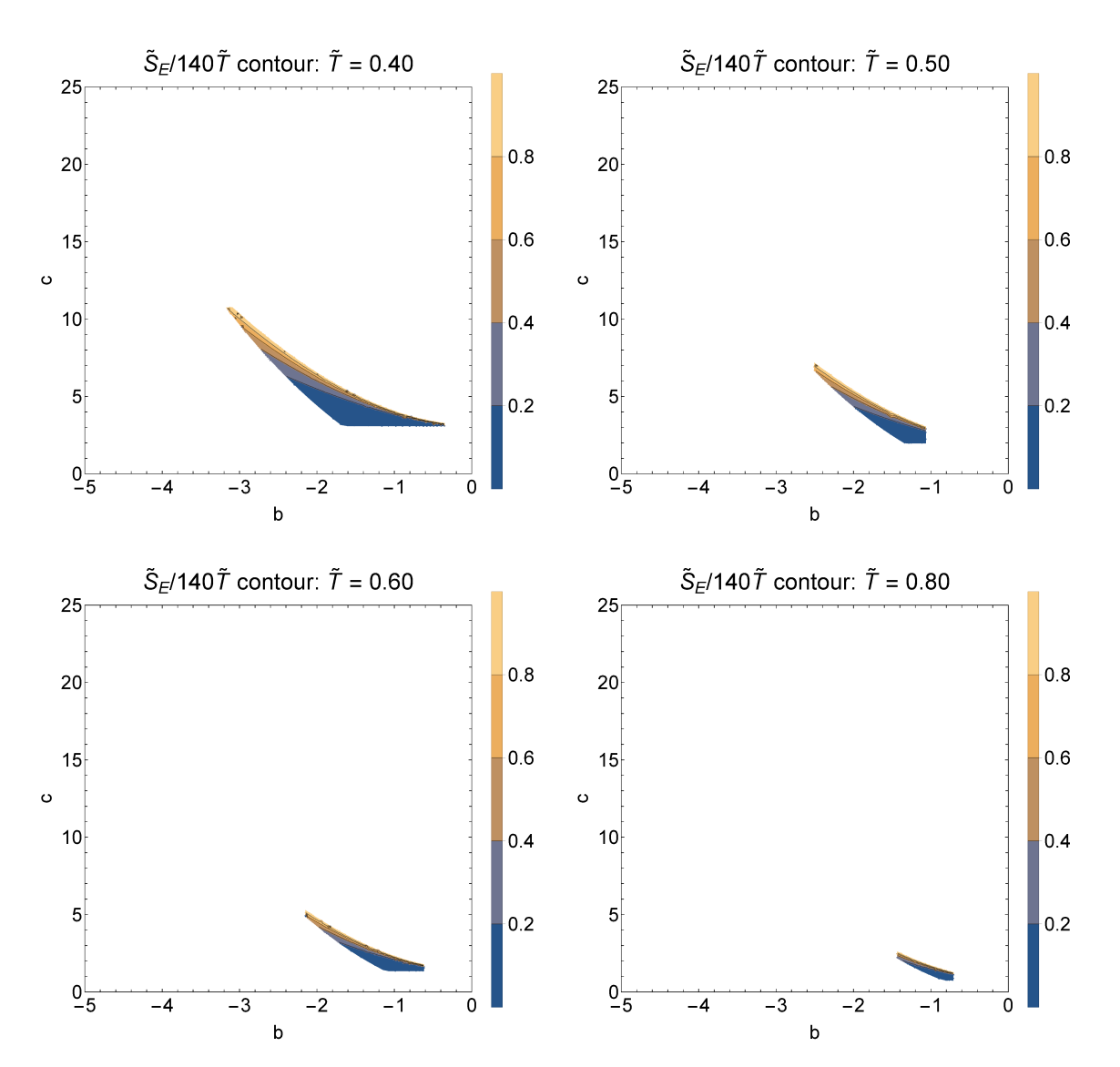


Figure 1. Contours of  $\tilde{S}_E/140\tilde{T}$  are shown in the (b,c) plane for smaller values of  $\tilde{T}$ :  $\tilde{T}=0.15$  (upper left), 0.20 (upper right), 0.25 (lower left), and 0.30 (lower right). The contours also satisfy the conditions:  $c \geq b^2$ ,  $c\tilde{T} \geq 1/2$ ,  $\alpha \leq 1$ ,  $0 \leq \tilde{S}_E/140\tilde{T} \leq 1$ ,  $\tilde{\beta}/H \geq \tilde{S}_E/140\tilde{T}$  and  $\tilde{\xi} \geq 0$ .

zero temperature through the relation  $(\Lambda/v)^2 = m/\sqrt{2}v$ . We thus see that these simple scaling arguments imply a powerful connection between gravitational wave observations of a cosmological phase transition and laboratory probes of the hidden sector at zero temperature. In particular, if the mass of the dark Higgs particle excitation is less than  $\mathcal{O}(1\%)$  of the dark Higgs vev, then the gravitational wave signal arising from condensation of the dark Higgs in the early Universe would have an amplitude too small to be observed at LISA. If the hidden sector is coupled to the Standard Model, then the dark Higgs mass and vev can be probed at fixed target or beam dump experiments, thus determining if a gravitational wave signal can be seen. Note that, although the maximum sensitivity of BBO will be 4–5 orders of magnitude better than LISA this leads to much less than an order of



**Figure 2.** Contours of  $\tilde{S}_E/140\tilde{T}$  are shown in the (b,c) plane for larger values of  $\tilde{T}$ :  $\tilde{T}=0.40$  (upper left), 0.50 (upper right), 0.60 (lower left), and 0.80 (lower right). The contours also satisfy the conditions:  $c \geq b^2$ ,  $c\tilde{T} \geq 1/2$ ,  $\alpha \leq 1$ ,  $0 \leq \tilde{S}_E/140\tilde{T} \leq 1$ ,  $\tilde{\beta}/H \geq \tilde{S}_E/140\tilde{T}$  and  $\tilde{\xi} \geq 0$ .

magnitude improvement in minimum value of m/v for models which can be probed with gravitational waves.

We can provide an even tighter bound on the amplitude of the gravitational wave signal by accounting for the dependence of  $h^2\Omega_{sw}^{\max}$  on  $\xi$  and  $\tilde{\beta}/H$ . In figure 7a, we scan over parameters  $(b,c,\Lambda/v)$ , plotting each point on the  $(h^2\Omega_{sw}^{\max},\Lambda/v)$ -plane. We have assumed  $v_w=1$ . If we could ignore the effects of supercooling, then we would expect from eq. (2.17) that the set of points with the largest values of  $h^2\Omega_{sw}^{\max}$  correspond to the choice of (b,c) for which  $h^2\tilde{\Omega}_{sw}^{\max}$  is largest, and lie along the line  $h^2\Omega_{sw}^{\max} \propto (\Lambda/v)^{18}$ . In fact, the slope of this line (plotted as the solid blue line in figure 7a) is  $\sim 17.2$ , which is only slightly different from that given above, indicating that the dependence of  $h^2\tilde{\Omega}_{sw}^{\max}$  on  $\Lambda/v$  induced

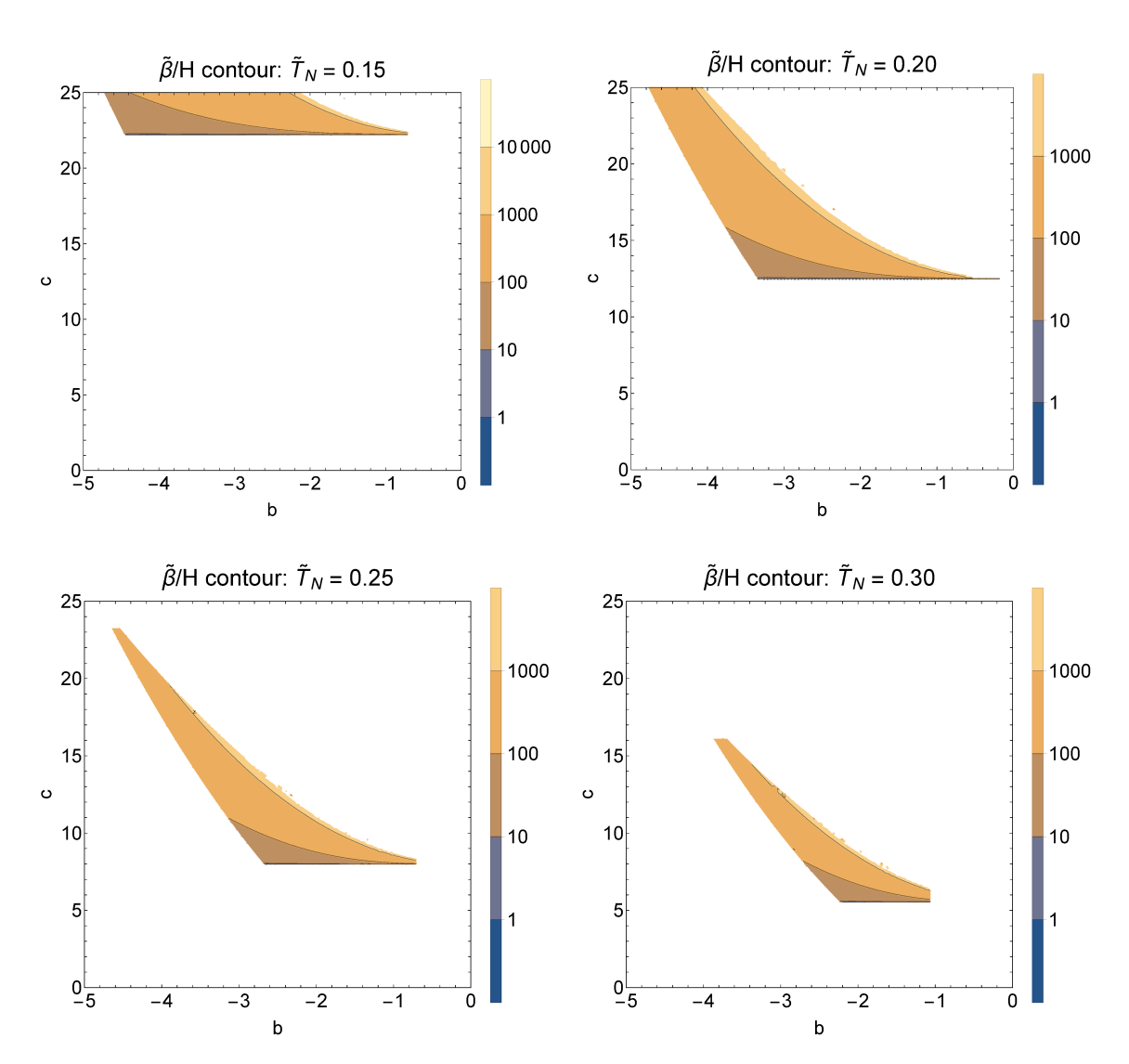


Figure 3. Contours of  $\tilde{\beta}/H$  are shown in the (b,c) plane for the allowed parameter space for lower values of  $\tilde{T}_N$ :  $\tilde{T}_N = 0.15$  (upper left), 0.20 (upper right), 0.25 (lower left), and 0.30 (lower right). The contours also satisfy the conditions:  $c \geq b^2$ ,  $c\tilde{T}_N \geq 1/2$ ,  $\alpha \leq 1$ ,  $0 \leq \tilde{S}_E/140\tilde{T}_N \leq 1$ ,  $\tilde{\beta}/H \geq \tilde{S}_E/140\tilde{T}_N$  and  $\tilde{\xi} \geq 0$ .

by the effects of supercooling is relatively minor. Similarly, in figure 7b, we scan over the parameters  $(b, c, \Lambda/v)$ , plotting each point in the  $(f_{sw}, \Lambda/v)$ -plane. Again, we see that most of the points roughly follow the  $f_{sw}/v \propto (\Lambda/v)^{-2}$  relation which we found earlier (ignoring the effects of supercooling), with a spread of roughly an order of magnitude in  $f_{sw}/v$  for any  $\Lambda/v$ .

In figure 8, we plot the set of points in the (b,c)-plane for which  $h^2\Omega_{sw}^{\max}$  is within 2% of the maximum for any given value of  $\Lambda/v$ . These points correspond to the (b,c) values of the points near the solid blue line in figure 7a, discussed above. We see that scatter in these points is small, another indication that the effects of supercooling are relatively minor (if these effects were negligible, then all parameter points on this line would have the

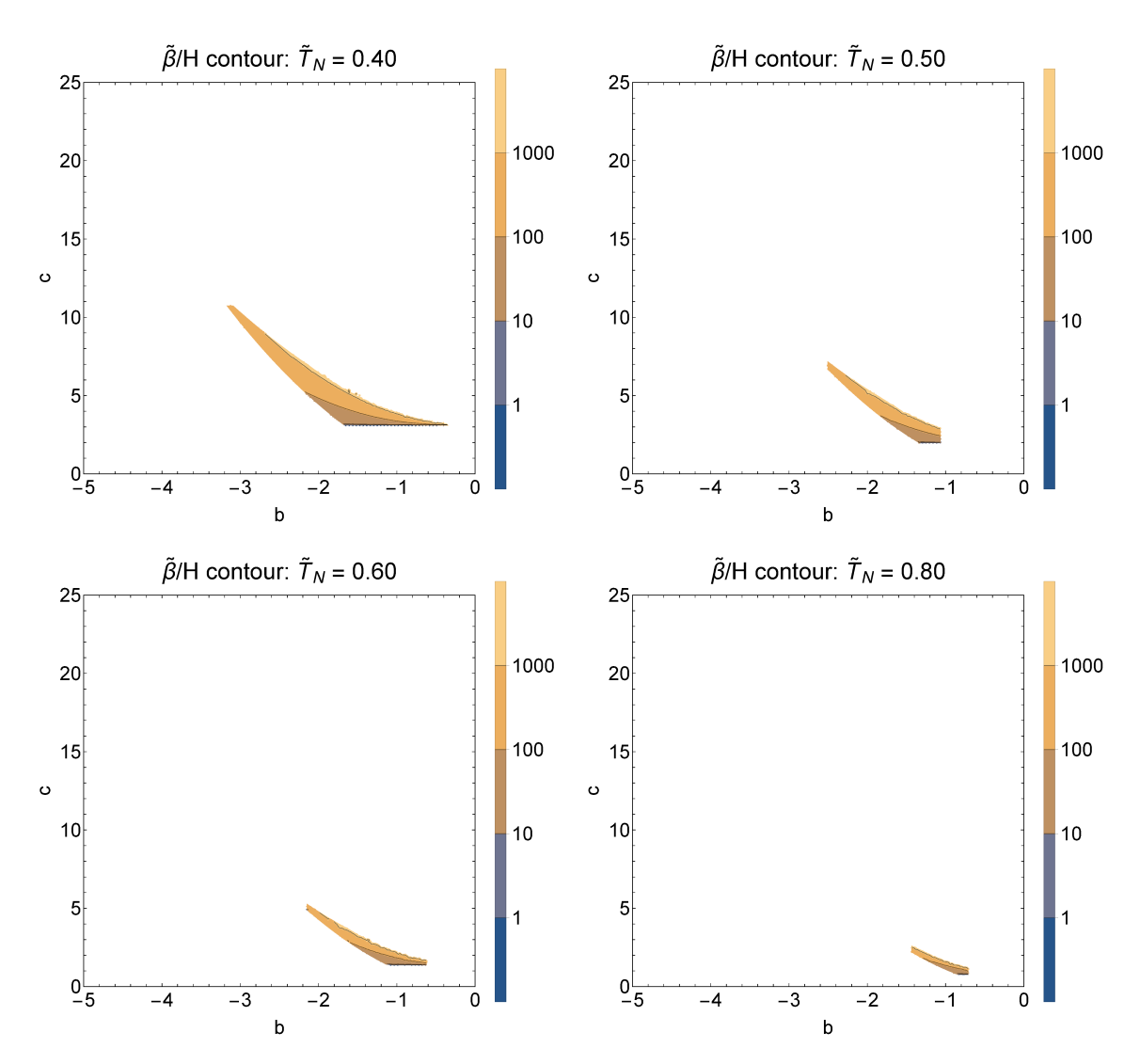


Figure 4. Contours of  $\tilde{\beta}/H$  are shown in the (b,c) plane for the allowed parameter space for higher values of  $\tilde{T}_N$ :  $\tilde{T}_N = 0.40$  (upper left), 0.50 (upper right), 0.60 (lower left), and 0.80 (lower right). The contours also satisfy the conditions:  $c \geq b^2$ ,  $c\tilde{T}_N \geq 1/2$ ,  $\alpha \leq 1$ ,  $0 \leq \tilde{S}_E/140\tilde{T}_N \leq 1$ ,  $\tilde{\beta}/H \geq \tilde{S}_E/140\tilde{T}_N$  and  $\tilde{\xi} \geq 0$ .

same values of b and c, differing only in the parameter  $\Lambda/v$ ). We also plot shaded regions indicating values of (b,c) for which a given nucleation temperature  $\tilde{T}_N$  can be realized. We see that these models with maximal signal amplitude can only be realized with  $\tilde{T}_N < 0.4$ .

Finally, in figure 9, we scan over models, which are plotted in ths  $(f_{sw}, h^2 \Omega_{sw}^{\max})$ -plane, taking  $v_w = 1$ . In particular, we scan over b, c, and  $\Lambda/v$ , with v = 1 MeV (brown), 100 GeV (green), 1 TeV (pink), and 1000 TeV (blue). We find  $f_{sw} \propto v$ , while for any choice of v, we roughly find  $h^2 \Omega_{sw}^{\max} \propto f_{sw}^{-9}$ , as one would expect from eq. (2.17). We also plot the sensitivity of a variety of current and upcoming gravitational wave observatories in figure 9.

Note that the most sensitive upcoming experiments (BBO and ALIA) will probe models with symmetry-breaking scales in the range  $\mathcal{O}(100-1000)$  GeV. For scenarios with new

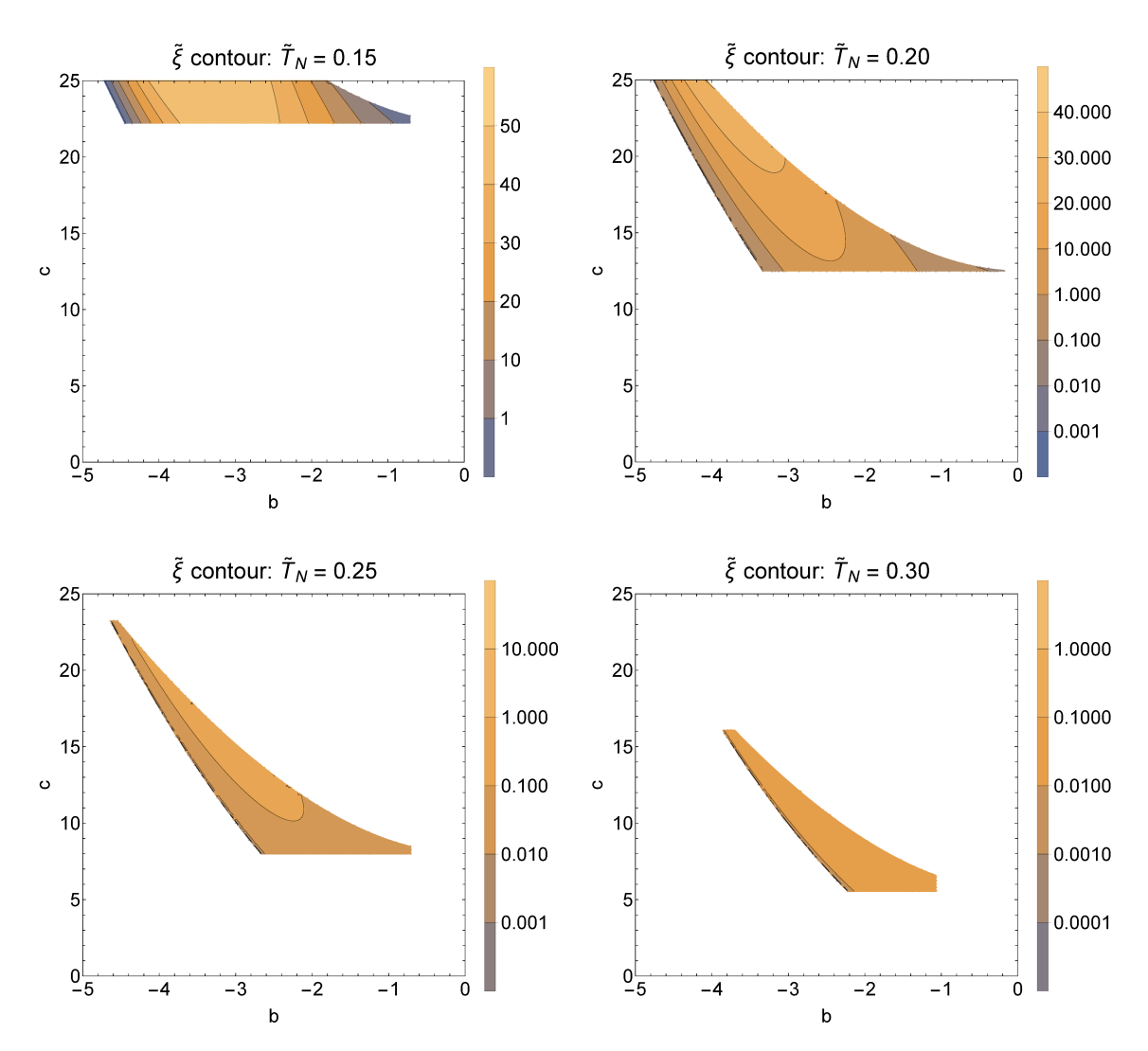


Figure 5. Contours of  $\tilde{\xi}$  are shown in the (b,c) plane for the allowed parameter space for lower values of  $\tilde{T}_N$ :  $\tilde{T}_N = 0.15$  (upper left), 0.20 (upper right), 0.25 (lower left), and 0.30 (lower right). The contours also satisfy the conditions:  $c \geq b^2$ ,  $c\tilde{T}_N \geq 1/2$ ,  $\alpha \leq 1$ ,  $0 \leq \tilde{S}_E/140\tilde{T}_N \leq 1$ ,  $\tilde{\beta}/H \geq \tilde{S}_E/140\tilde{T}_N$  and  $\tilde{\xi} \geq 0$ .

physics appearing at the MeV-scale, experiments such as THEIA would provide the leading sensitivity, while for scenarios with new physics appearing at the PeV-scale, experiments such as ET and CE would provide the leading sensitivity. But the absence of sensitivity for models with  $m/v < \mathcal{O}(0.01)$  is largely independent of scale; even at the scales for which future experiments will be most sensitive, this lower bound can be reduced by no more than a factor of a few. These experiments are described in table 1.

Note from figure 7a that, although the upper bound on  $h^2\Omega_{sw}^{max}$  follows fairly closely the scaling relations we have derived, and in particular, grows steeply with  $\Lambda/v$ , the actual amplitude may be much smaller than this maximum. For example, the behavior of the SM electroweak phase transition is different, with the amplitude of a gravitational wave signal decreasing with  $m_h/v$ , and disappearing entirely for  $m_h = 125$  GeV, at which point the phase transition is smooth. This is because the thermal effective potential for the Standard

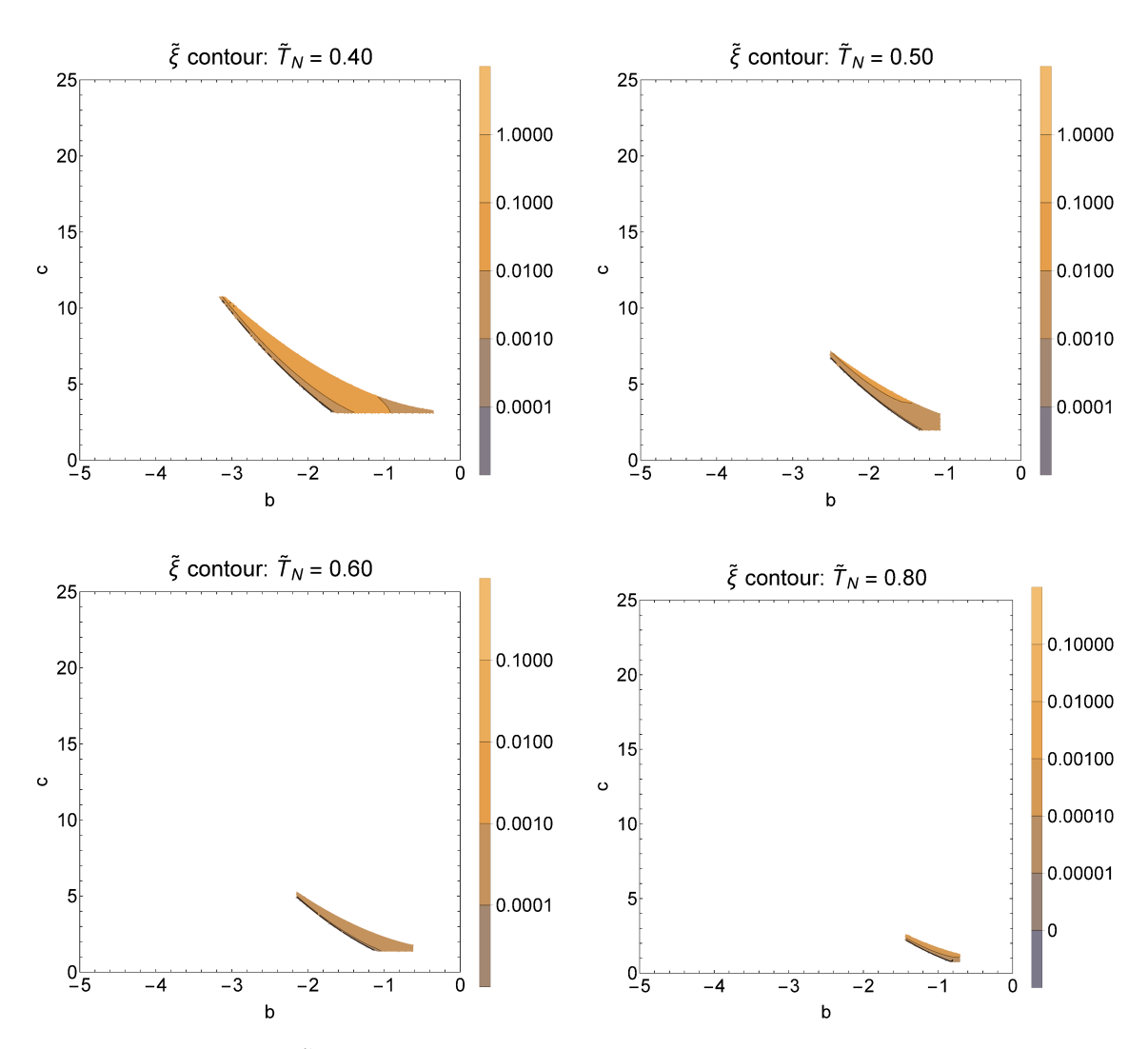


Figure 6. Contours of  $\tilde{\xi}$  are shown in the (b,c) plane for the allowed parameter space for higher values of  $\tilde{T}_N$ :  $\tilde{T}_N = 0.40$  (upper left), 0.50 (upper right), 0.60 (lower left), and 0.80 (lower right). The contours also satisfy the conditions:  $c \geq b^2$ ,  $c\tilde{T}_N \geq 1/2$ ,  $\alpha \leq 1$ ,  $0 \leq \tilde{S}_E/140\tilde{T}_N \leq 1$ ,  $\tilde{\beta}/H \geq \tilde{S}_E/140\tilde{T}_N$  and  $\tilde{\xi} \geq 0$ .

Model Higgs sector corresponds to a choice of parameters which lie well below the upper bound on  $h^2\Omega_{sw}^{\rm max}$ . For sufficiently large  $m_h/v$ , the parameter c becomes small enough that the potential barrier disappears before reaching the nucleation temperature. This example illustrates the point that, although this analysis provides an upper limit on the gravitational wave signal, it would be much more difficult to translate a measurement of m/v into a prediction for the gravitational wave amplitude, or vice versa.

# 4 Conclusions

We have considered gravitational wave signals from sound waves in the context of an effective field theory with a renormalizable thermal potential exhibiting a first-order phase transition

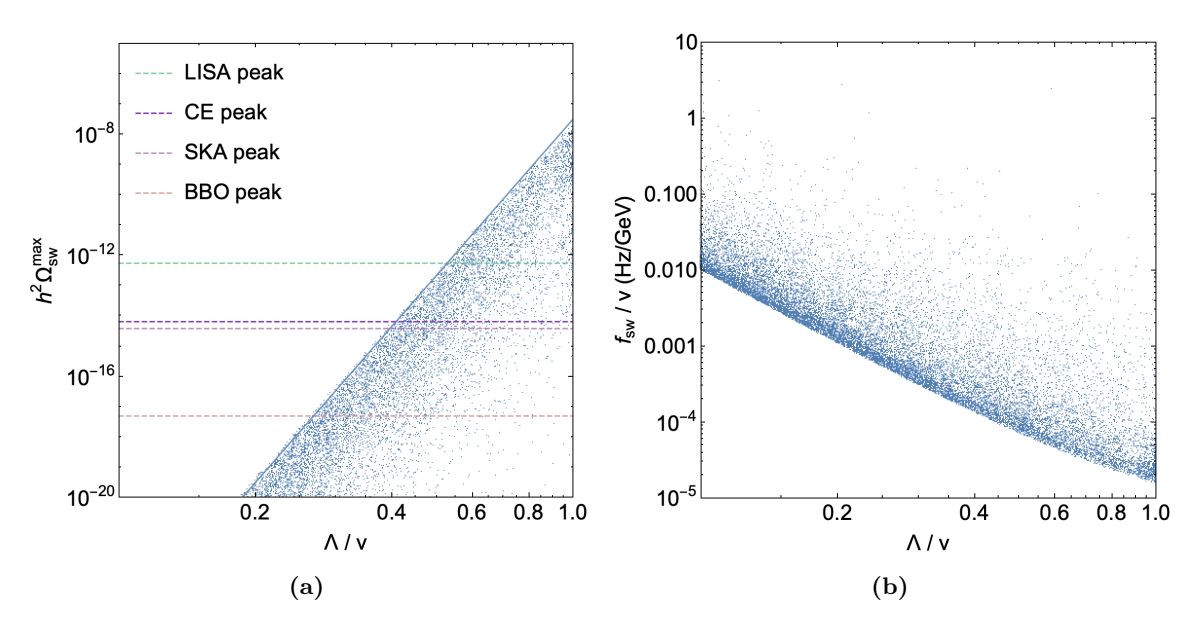


Figure 7. Plot of  $h^2\Omega_{sw}^{\max}$  (left) and  $f_{sw}/v$  (right) against  $\Lambda/v$  for a set of models obtained by scanning of  $0 \le \Lambda/v \le 1$ ,  $-5 \le b \le 0$  and  $0 \le c \le 25$ . The dashed lines in the left panel are the maximum sensitivities of LISA (green), BBO (beige), SKA (magenta) and CE (purple). The solid blue line in the left panel presents the maximum value of  $h^2\Omega_{sw}^{\max}$  obtained for a given  $\Lambda/v$ , for any (b,c); this line has a slope of  $\sim 17.2$ .

in the early Universe. We have considered a thermal effective potential of power law form, which would arise, for example, in the high temperature limit. This approach allows us to consider the gravitational wave signals produced by phase transitions in a wide class of models.

We find that for this class of models, there is a relatively clean relationship between the parameters of the gravitational wave signal and the parameters of the thermal effective potential. The effective potential can be expressed in terms of one dimensionful parameter, the vacuum expectation value of the dark Higgs (v), which sets the frequency scale of the gravitational wave signal. The amplitude of the gravitational wave signal is largely set by one dimensionless parameter,  $\Lambda/v$ , which sets the ratio of the potential energy scale to the dark Higgs vev. Since the amplitude of the gravitational wave signal scales as  $\Lambda/v$  to a very high power, the dependence on the other dimensionless parameters is subdominant.

This approach leads to a striking conclusion. If the ratio of the dark Higgs mass to the dark Higgs vev is less than  $\mathcal{O}(10^{-2})$ , then the magnitude of the gravitational wave signal will be so small as to be undetectable by any upcoming observatories. This bound on sensitivity is nearly independent of the scale of new physics. This result is also robust against future developments in our understanding of the amplitude of gravitational sound waves produced by a first-order cosmological phase transition. Since the amplitude depends on  $m_f/v$  raised to a high power, to modify our bound by an order of magnitude would require a new correction to the sound wave amplitude of several orders of magnitude.

This result leads to several intriguing possibilities. For example, in scenarios of new MeV-scale physics, one may potentially be able to probe the symmetry-breaking scale with

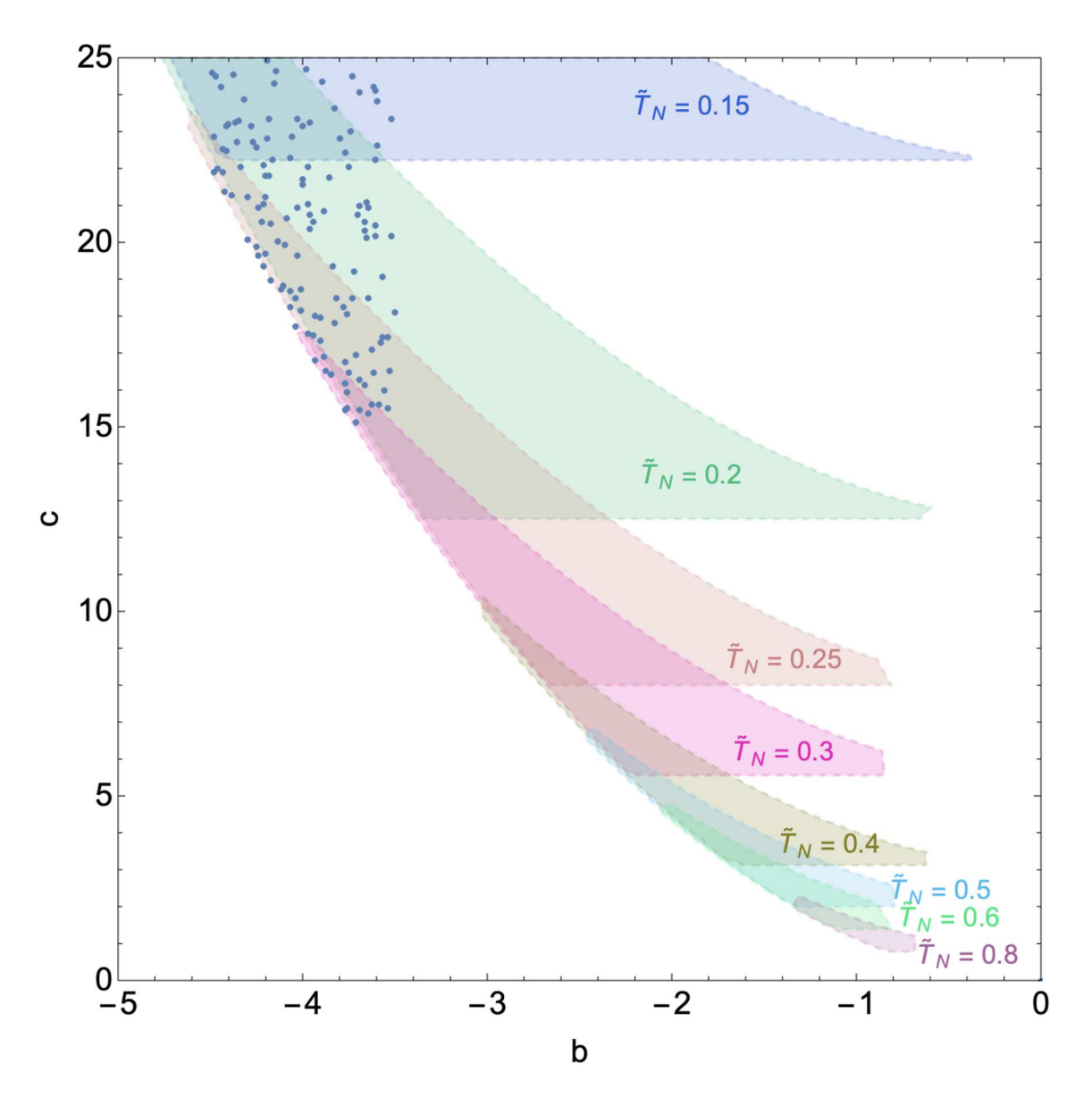


Figure 8. Plot in the (b, c)-plane of parameter points for which  $h^2\Omega_{sw}^{\max}$  is within 2% of solid blue line shown in figure 7a. The shaded regions indicate regions in the (b, c)-plane for which various nucleation temperatures  $\tilde{T}_N$  can be realized.

forward detectors at high-luminosity beam experiments, which could potentially determine the mass and coupling of the dark photon. The detection of a gravitational wave signal from the corresponding first-order phase transition would then provide a lower bound on the Higgs mass. Similarly, it is possible that future high-energy beam experiments could produce a heavy ( $> \mathcal{O}(\text{TeV})$ ) dark Higgs. In this case, the amplitude of a gravitational wave signal from the phase transition would correspond to an upper bound on the symmetry-breaking scale.

There are several avenues for further exploration. We have considered a power-law form for the thermal effective potential, which is expected to be a good approximation for renormalizable models, in the high-temperature limit. But there are a variety of models in which the phase transition is supercooled (see, for example [177–180]), and nucleation

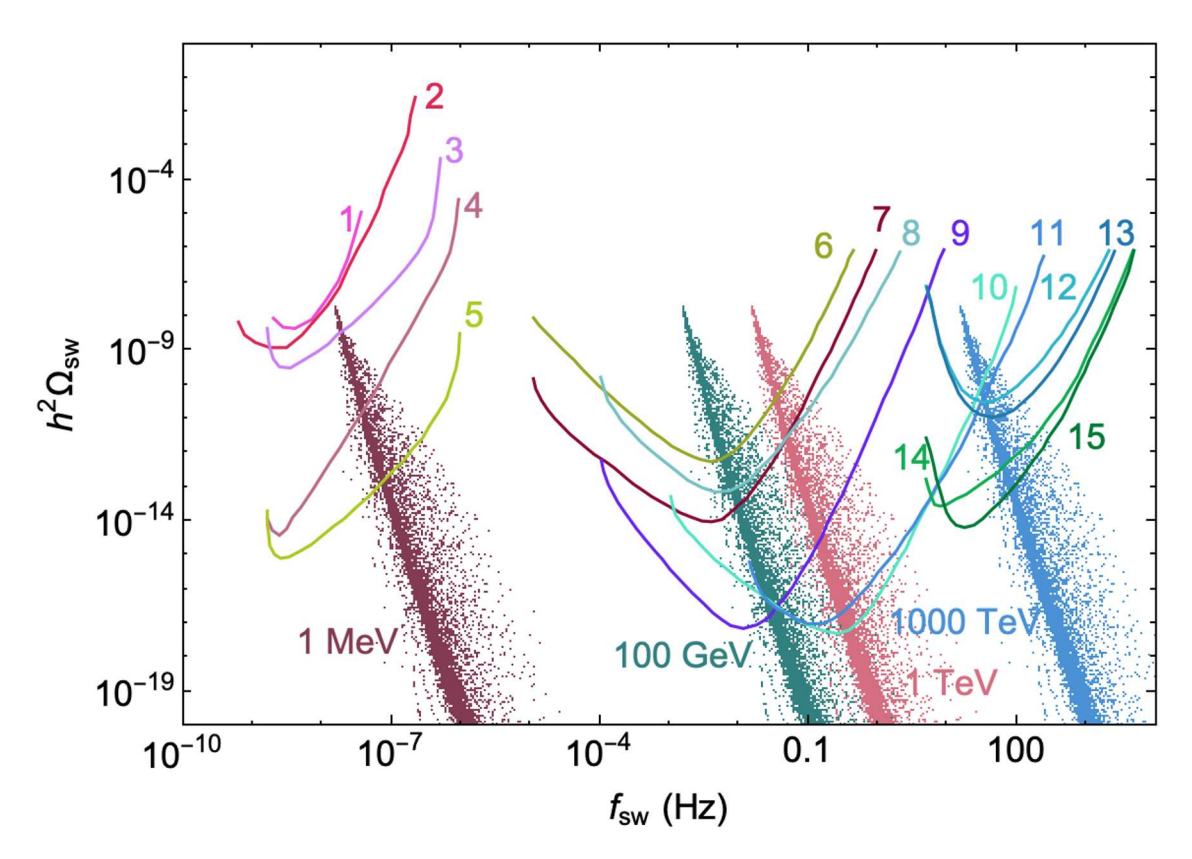


Figure 9. Plot in the  $(h^2\Omega_{sw}, f_{sw})$ -plane of the gravitational wave signal obtained from a scan of parameter points  $(b, c, \Lambda/v)$ . The values of v used are 1 MeV, 100 GeV, 1 TeV and 1000 TeV (from left to right). Also plotted are the sensitivities of the following current and upcoming experiments: 1. EPTA [156], 2. NANOGrav [157, 158], 3. Gaia [159], 4. SKA [160], 5. THEIA [161], 6. LISA [12, 162, 163], 7. Taiji [164], 8.TianQin [165], 9. ALIA [166], 10. BBO [167, 168], 11. DE-CIGO [169, 170], 12. aLIGO [171, 172], 13. A+ [173], 14. ET [174], 15. CE [175].

temperature is relatively low. In these cases, although the corrections to the form of the potential may be small, they need not be. There has been significant recent work regarding theoretical issues in finite temperature perturbation theory (see, for example, [145, 181]).

Similarly, we have assumed that the thermal effective potential is renormalizable. There are interesting models of new physics in which the phase transition can only be seen with the inclusion of non-renormalizable terms. It would be interesting to consider more general forms of the thermal effective potential, to better determine the extent to which the lessons found here generalize.

## Acknowledgments

We are grateful to Djuna Croon, Jeremy Sakstein, Tim Tait, and especially Graham White for useful discussions. The work of JK is supported in part by DOE grant DE-SC0010504. JR is supported by NSF grant AST-1934744. The work of BD and SG is supported in part by DOE grant DE-SC0010813. The work of SG is also supported in part by National Research Foundation of Korea (NRF) Grant No. NRF-2019R1A2C3005009 (SG). JBD acknowledges support from the National Science Foundation under grants no. PHY-1820801 and PHY-1748958.

Classifications based on frequency reach	Dark sector scale that can be probed	Type of experiments	Experiments
			EPTA (European Pulsar Timing Array) [156]
Very low frequency $10^{-9} - 10^{-8}$ Hz	$\leq 1  \mathrm{MeV}$	Ground-based telescope using pulsar timing observation technique	NANOGrav (North American Nanohertz Observatory for Gravitational Wave) [157, 158]
			SKA (Square Kilometer Array) [160]: World's largest radio telescope
			Gaia [159]
		Space-based telescope using astrometry	THEIA (Telescope for Habitable Exoplanets and Intersteller/Intergalactic Astronomy) [161]: Proposed upgrade of Gaia
$\mu$ -frequency $10^{-6} - 10^{-5} \text{ Hz}$	$\sim 100\mathrm{MeV}$	Space-based heliocentric constellation of satellites using Laser interferometry technique	$\mu ext{-Ares}$ [176]
		Space-based interferometer using Laser interferometry technique	LISA (Laser Interferometer Space Antenna) [12, 162, 163]
			ALIA (Advanced Laser Interferometer Antenna) [166]
	100 GeV-1 TeV		Taiji [164]
Low frequency $10^{-3} - 1 \text{ Hz}$			TianQin [165]
			BBO (Big Bang Observer) [167, 168]
			DECIGO (Deci-Hertz Interferometer Gravitational Wave Observatory) [169, 170]

**Table 1.** Description of upcoming gravitational wave observatories, including the frequency range to which they would be sensitive, and the correspond symmetry-breaking scale (continues).

Classifications based on frequency reach	Dark sector scale that can be probed	Type of experiments	Experiments
High frequency 10 - 100 Hz	∼1000 TeV	Second generation Ground-based interferometer using Laser interferometry technique	aLIGO (Advanced LIGO) [171, 172] $A + [173] \; (Quantum \; LIGO)$
		Third generation Ground-based interferometer using Laser interferometry technique	ET (Einstein Telescope) [174] CE (Cosmic Explorer) [175]

**Table 1.** Description of upcoming gravitational wave observatories, including the frequency range to which they would be sensitive, and the correspond symmetry-breaking scale.

**Open Access.** This article is distributed under the terms of the Creative Commons Attribution License (CC-BY 4.0), which permits any use, distribution and reproduction in any medium, provided the original author(s) and source are credited. SCOAP<sup>3</sup> supports the goals of the International Year of Basic Sciences for Sustainable Development.

## References

- [1] LIGO SCIENTIFIC and VIRGO collaborations, Observation of Gravitational Waves from a Binary Black Hole Merger, Phys. Rev. Lett. 116 (2016) 061102 [arXiv:1602.03837] [INSPIRE].
- [2] A. Kosowsky, M.S. Turner and R. Watkins, *Gravitational waves from first order cosmological phase transitions*, *Phys. Rev. Lett.* **69** (1992) 2026 [INSPIRE].
- [3] A. Kosowsky, M.S. Turner and R. Watkins, Gravitational radiation from colliding vacuum bubbles, Phys. Rev. D 45 (1992) 4514 [INSPIRE].
- [4] R. Apreda, M. Maggiore, A. Nicolis and A. Riotto, *Gravitational waves from electroweak phase transitions*, *Nucl. Phys. B* **631** (2002) 342 [gr-qc/0107033] [INSPIRE].
- [5] C. Grojean and G. Servant, Gravitational Waves from Phase Transitions at the Electroweak Scale and Beyond, Phys. Rev. D 75 (2007) 043507 [hep-ph/0607107] [INSPIRE].
- [6] S.J. Huber and T. Konstandin, Gravitational Wave Production by Collisions: More Bubbles, JCAP 09 (2008) 022 [arXiv:0806.1828] [INSPIRE].
- [7] R.-G. Cai, Z. Cao, Z.-K. Guo, S.-J. Wang and T. Yang, *The Gravitational-Wave Physics*, Natl. Sci. Rev. 4 (2017) 687 [arXiv:1703.00187] [INSPIRE].
- [8] D.J. Weir, Gravitational waves from a first order electroweak phase transition: a brief review, Phil. Trans. Roy. Soc. Lond. A 376 (2018) 20170126 [arXiv:1705.01783] [INSPIRE].
- [9] C. Caprini et al., Science with the space-based interferometer eLISA. II: Gravitational waves from cosmological phase transitions, JCAP 04 (2016) 001 [arXiv:1512.06239] [INSPIRE].

- [10] A. Mazumdar and G. White, Review of cosmic phase transitions: their significance and experimental signatures, Rept. Prog. Phys. 82 (2019) 076901 [arXiv:1811.01948] [INSPIRE].
- [11] C. Caprini and D.G. Figueroa, Cosmological Backgrounds of Gravitational Waves, Class. Quant. Grav. 35 (2018) 163001 [arXiv:1801.04268] [INSPIRE].
- [12] C. Caprini et al., Detecting gravitational waves from cosmological phase transitions with LISA: an update, JCAP 03 (2020) 024 [arXiv:1910.13125] [INSPIRE].
- [13] R. Caldwell et al., Detection of Early-Universe Gravitational Wave Signatures and Fundamental Physics, arXiv:2203.07972 [INSPIRE].
- [14] A. Ashoorioon and T. Konstandin, Strong electroweak phase transitions without collider traces, JHEP 07 (2009) 086 [arXiv:0904.0353] [INSPIRE].
- [15] A. Alves, T. Ghosh, H.-K. Guo, K. Sinha and D. Vagie, Collider and Gravitational Wave Complementarity in Exploring the Singlet Extension of the Standard Model, JHEP 04 (2019) 052 [arXiv:1812.09333] [INSPIRE].
- [16] C. Balázs, A. Fowlie, A. Mazumdar and G. White, Gravitational waves at aLIGO and vacuum stability with a scalar singlet extension of the Standard Model, Phys. Rev. D 95 (2017) 043505 [arXiv:1611.01617] [INSPIRE].
- [17] Z. Kang, P. Ko and T. Matsui, Strong first order EWPT & strong gravitational waves in Z<sub>3</sub>-symmetric singlet scalar extension, JHEP **02** (2018) 115 [arXiv:1706.09721] [INSPIRE].
- [18] T. Matsui, Gravitational waves from the first order electroweak phase transition in the Z<sub>3</sub> symmetric singlet scalar model, EPJ Web Conf. 168 (2018) 05001 [arXiv:1709.05900] [INSPIRE].
- [19] V. Vaskonen, Electroweak baryogenesis and gravitational waves from a real scalar singlet, Phys. Rev. D 95 (2017) 123515 [arXiv:1611.02073] [INSPIRE].
- [20] M. Lewicki, M. Merchand and M. Zych, Electroweak bubble wall expansion: gravitational waves and baryogenesis in Standard Model-like thermal plasma, JHEP 02 (2022) 017 [arXiv:2111.02393] [INSPIRE].
- [21] D. Croon and G. White, Exotic Gravitational Wave Signatures from Simultaneous Phase Transitions, JHEP 05 (2018) 210 [arXiv:1803.05438] [INSPIRE].
- [22] A. Beniwal, M. Lewicki, M. White and A.G. Williams, Gravitational waves and electroweak baryogenesis in a global study of the extended scalar singlet model, JHEP **02** (2019) 183 [arXiv:1810.02380] [INSPIRE].
- [23] K. Hashino, R. Jinno, M. Kakizaki, S. Kanemura, T. Takahashi and M. Takimoto, Selecting models of first-order phase transitions using the synergy between collider and gravitational-wave experiments, Phys. Rev. D 99 (2019) 075011 [arXiv:1809.04994] [INSPIRE].
- [24] A. Ahriche, K. Hashino, S. Kanemura and S. Nasri, Gravitational Waves from Phase Transitions in Models with Charged Singlets, Phys. Lett. B 789 (2019) 119 [arXiv:1809.09883] [INSPIRE].
- [25] V.R. Shajiee and A. Tofighi, Electroweak Phase Transition, Gravitational Waves and Dark Matter in Two Scalar Singlet Extension of The Standard Model, Eur. Phys. J. C 79 (2019) 360 [arXiv:1811.09807] [INSPIRE].
- [26] T. Vieu, A.P. Morais and R. Pasechnik, Electroweak phase transitions in multi-Higgs models: the case of Trinification-inspired THDSM, JCAP 07 (2018) 014 [arXiv:1801.02670] [INSPIRE].

- [27] A. Alves, T. Ghosh, H.-K. Guo and K. Sinha, Resonant Di-Higgs Production at Gravitational Wave Benchmarks: A Collider Study using Machine Learning, JHEP 12 (2018) 070 [arXiv:1808.08974] [INSPIRE].
- [28] M. Chala, M. Ramos and M. Spannowsky, Gravitational wave and collider probes of a triplet Higgs sector with a low cutoff, Eur. Phys. J. C 79 (2019) 156 [arXiv:1812.01901] [INSPIRE].
- [29] K. Fujikura, K. Kamada, Y. Nakai and M. Yamaguchi, *Phase Transitions in Twin Higgs Models*, *JHEP* **12** (2018) 018 [arXiv:1810.00574] [INSPIRE].
- [30] L. Gráf, S. Jana, A. Kaladharan and S. Saad, Gravitational wave imprints of left-right symmetric model with minimal Higgs sector, JCAP 05 (2022) 003 [arXiv:2112.12041] [INSPIRE].
- [31] M. Li, Q.-S. Yan, Y. Zhang and Z. Zhao, Prospects of gravitational waves in the minimal left-right symmetric model, JHEP 03 (2021) 267 [arXiv:2012.13686] [INSPIRE].
- [32] P.H. Ghorbani, Electroweak phase transition in the scale invariant standard model, Phys. Rev. D 98 (2018) 115016 [arXiv:1711.11541] [INSPIRE].
- [33] C. Marzo, L. Marzola and V. Vaskonen, *Phase transition and vacuum stability in the classically conformal B-L model*, *Eur. Phys. J. C* **79** (2019) 601 [arXiv:1811.11169] [INSPIRE].
- [34] L. Marzola, A. Racioppi and V. Vaskonen, Phase transition and gravitational wave phenomenology of scalar conformal extensions of the Standard Model, Eur. Phys. J. C 77 (2017) 484 [arXiv:1704.01034] [INSPIRE].
- [35] D. Verweij, On the construction and measurement of conformal extensions of the Standard Model, MSc. Thesis, Utrecht University, Utrecht, Netherlands (2019).
- [36] T. Prokopec, J. Rezacek and B. Świeżewska, *Gravitational waves from conformal symmetry breaking*, *JCAP* **02** (2019) 009 [arXiv:1809.11129] [INSPIRE].
- [37] R. Zhou, W. Cheng, X. Deng, L. Bian and Y. Wu, Electroweak phase transition and Higgs phenomenology in the Georgi-Machacek model, JHEP **01** (2019) 216 [arXiv:1812.06217] [INSPIRE].
- [38] P. Archer-Smith, D. Linthorne and D. Stolarski, *Gravitational Wave Signals from Multiple Hidden Sectors*, *Phys. Rev. D* **101** (2020) 095016 [arXiv:1910.02083] [INSPIRE].
- [39] R.-G. Cai, K. Hashino, S.-J. Wang and J.-H. Yu, Gravitational waves from patterns of electroweak symmetry breaking: an effective perspective, arXiv:2202.08295 [INSPIRE].
- [40] A. Paul, U. Mukhopadhyay and D. Majumdar, Gravitational Wave Signatures from Domain Wall and Strong First-Order Phase Transitions in a Two Complex Scalar extension of the Standard Model, JHEP 05 (2021) 223 [arXiv:2010.03439] [INSPIRE].
- [41] W. Chao, W.-F. Cui, H.-K. Guo and J. Shu, Gravitational wave imprint of new symmetry breaking, Chin. Phys. C 44 (2020) 123102 [arXiv:1707.09759] [INSPIRE].
- [42] E.M. Pimentel, *Phenomenology of New Physics Models at Colliders and in Gravitational Waves*, Ph.D. Thesis, Mainz University, Mainz, Germany (2020) [DOI].
- [43] N. Blinov, J. Kozaczuk, D.E. Morrissey and C. Tamarit, *Electroweak Baryogenesis from Exotic Electroweak Symmetry Breaking*, *Phys. Rev. D* **92** (2015) 035012 [arXiv:1504.05195] [INSPIRE].
- [44] S. Inoue, G. Ovanesyan and M.J. Ramsey-Musolf, Two-Step Electroweak Baryogenesis, Phys. Rev. D 93 (2016) 015013 [arXiv:1508.05404] [INSPIRE].

- [45] A. Greljo, T. Opferkuch and B.A. Stefanek, Gravitational Imprints of Flavor Hierarchies, Phys. Rev. Lett. 124 (2020) 171802 [arXiv:1910.02014] [INSPIRE].
- [46] D. Croon, T.E. Gonzalo and G. White, Gravitational Waves from a Pati-Salam Phase Transition, JHEP 02 (2019) 083 [arXiv:1812.02747] [INSPIRE].
- [47] S.V. Demidov, D.S. Gorbunov and D.V. Kirpichnikov, Gravitational waves from phase transition in split NMSSM, Phys. Lett. B 779 (2018) 191 [arXiv:1712.00087] [INSPIRE].
- [48] L. Bian, H.-K. Guo and J. Shu, Gravitational Waves, baryon asymmetry of the universe and electric dipole moment in the CP-violating NMSSM, Chin. Phys. C 42 (2018) 093106 [Erratum ibid. 43 (2019) 129101] [arXiv:1704.02488] [INSPIRE].
- [49] A. Eichhorn, J. Lumma, J.M. Pawlowski, M. Reichert and M. Yamada, *Universal gravitational-wave signatures from heavy new physics in the electroweak sector*, *JCAP* **05** (2021) 006 [arXiv:2010.00017] [INSPIRE].
- [50] K. Miura, H. Ohki, S. Otani and K. Yamawaki, Gravitational Waves from Walking Technicolor, JHEP 10 (2019) 194 [arXiv:1811.05670] [INSPIRE].
- [51] A. Azatov, D. Barducci and F. Sgarlata, Gravitational traces of broken gauge symmetries, JCAP 07 (2020) 027 [arXiv:1910.01124] [INSPIRE].
- [52] M. Aoki, H. Goto and J. Kubo, Gravitational Waves from Hidden QCD Phase Transition, Phys. Rev. D 96 (2017) 075045 [arXiv:1709.07572] [INSPIRE].
- [53] Y. Chen, M. Huang and Q.-S. Yan, Gravitation waves from QCD and electroweak phase transitions, JHEP 05 (2018) 178 [arXiv:1712.03470] [INSPIRE].
- [54] D. Croon, J.N. Howard, S. Ipek and T.M.P. Tait, QCD baryogenesis, Phys. Rev. D 101 (2020) 055042 [arXiv:1911.01432] [INSPIRE].
- [55] D. Croon, R. Houtz and V. Sanz, Dynamical Axions and Gravitational Waves, JHEP 07 (2019) 146 [arXiv:1904.10967] [INSPIRE].
- [56] F. Costa, S. Khan and J. Kim, A two-component dark matter model and its associated gravitational waves, JHEP 06 (2022) 026 [arXiv:2202.13126] [INSPIRE].
- [57] W. Chao, H.-K. Guo and J. Shu, Gravitational Wave Signals of Electroweak Phase Transition Triggered by Dark Matter, JCAP 09 (2017) 009 [arXiv:1702.02698] [INSPIRE].
- [58] T. Ghosh, H.-K. Guo, T. Han and H. Liu, Electroweak phase transition with an SU(2) dark sector, JHEP 07 (2021) 045 [arXiv:2012.09758] [INSPIRE].
- [59] W. Chao, H.-K. Guo and X.-F. Li, First Order Color Symmetry Breaking and Restoration Triggered by Electroweak Symmetry Non-restoration, arXiv:2112.13580 [INSPIRE].
- [60] A. Romero et al., Implications for First-Order Cosmological Phase Transitions from the Third LIGO-Virgo Observing Run, Phys. Rev. Lett. 126 (2021) 151301 [arXiv:2102.01714] [INSPIRE].
- [61] A. Alves, D. Gonçalves, T. Ghosh, H.-K. Guo and K. Sinha, *Di-Higgs Blind Spots in Gravitational Wave Signals*, *Phys. Lett. B* **818** (2021) 136377 [arXiv:2007.15654] [INSPIRE].
- [62] E. Hall, T. Konstandin, R. McGehee, H. Murayama and G. Servant, *Baryogenesis From a Dark First-Order Phase Transition*, *JHEP* **04** (2020) 042 [arXiv:1910.08068] [INSPIRE].
- [63] E. Hall, T. Konstandin, R. McGehee and H. Murayama, Asymmetric Matters from a Dark First-Order Phase Transition, arXiv:1911.12342 [INSPIRE].

- [64] E. Madge and P. Schwaller, Leptophilic dark matter from gauged lepton number: Phenomenology and gravitational wave signatures, JHEP 02 (2019) 048 [arXiv:1809.09110] [INSPIRE].
- [65] D. Croon, V. Sanz and G. White, Model Discrimination in Gravitational Wave spectra from Dark Phase Transitions, JHEP 08 (2018) 203 [arXiv:1806.02332] [INSPIRE].
- [66] K. Hashino, M. Kakizaki, S. Kanemura, P. Ko and T. Matsui, Gravitational waves from first order electroweak phase transition in models with the  $U(1)_X$  gauge symmetry, JHEP 06 (2018) 088 [arXiv:1802.02947] [INSPIRE].
- [67] P. Schwaller, Gravitational Waves from a Dark Phase Transition, Phys. Rev. Lett. 115 (2015) 181101 [arXiv:1504.07263] [INSPIRE].
- [68] T. Alanne, K. Tuominen and V. Vaskonen, Strong phase transition, dark matter and vacuum stability from simple hidden sectors, Nucl. Phys. B 889 (2014) 692 [arXiv:1407.0688] [INSPIRE].
- [69] A. Addazi and A. Marciano, Gravitational waves from dark first order phase transitions and dark photons, Chin. Phys. C 42 (2018) 023107 [arXiv:1703.03248] [INSPIRE].
- [70] M. Fairbairn, E. Hardy and A. Wickens, *Hearing without seeing: gravitational waves from hot and cold hidden sectors*, *JHEP* **07** (2019) 044 [arXiv:1901.11038] [INSPIRE].
- [71] G. Bertone et al., Gravitational wave probes of dark matter: challenges and opportunities, SciPost Phys. Core 3 (2020) 007 [arXiv:1907.10610] [INSPIRE].
- [72] F. Huang, V. Sanz, J. Shu and X. Xue, *LIGO as a probe of dark sectors*, *Phys. Rev. D* **104** (2021) 095001 [arXiv:2102.03155] [INSPIRE].
- [73] J. Halverson, C. Long, A. Maiti, B. Nelson and G. Salinas, *Gravitational waves from dark Yang-Mills sectors*, *JHEP* **05** (2021) 154 [arXiv:2012.04071] [INSPIRE].
- [74] Y. Nakai, M. Suzuki, F. Takahashi and M. Yamada, Gravitational Waves and Dark Radiation from Dark Phase Transition: Connecting NANOGrav Pulsar Timing Data and Hubble Tension, Phys. Lett. B 816 (2021) 136238 [arXiv:2009.09754] [INSPIRE].
- [75] W. Ratzinger and P. Schwaller, Whispers from the dark side: Confronting light new physics with NANOGrav data, SciPost Phys. 10 (2021) 047 [arXiv:2009.11875] [INSPIRE].
- [76] A. Bhoonah, J. Bramante, S. Nerval and N. Song, Gravitational Waves From Dark Sectors, Oscillating Inflatons, and Mass Boosted Dark Matter, JCAP 04 (2021) 043 [arXiv:2008.12306] [INSPIRE].
- [77] A.J. Helmboldt, J. Kubo and S. van der Woude, Observational prospects for gravitational waves from hidden or dark chiral phase transitions, Phys. Rev. D 100 (2019) 055025 [arXiv:1904.07891] [INSPIRE].
- [78] A. Beniwal, M. Lewicki, J.D. Wells, M. White and A.G. Williams, Gravitational wave, collider and dark matter signals from a scalar singlet electroweak baryogenesis, JHEP 08 (2017) 108 [arXiv:1702.06124] [INSPIRE].
- [79] I. Baldes, Generation of Asymmetric Dark Matter and Gravitational Waves, in 29th Rencontres de Blois on Particle Physics and Cosmology, Blois, France, 28 May-2 June 2017 [arXiv:1711.08251] [INSPIRE].
- [80] I. Baldes and C. Garcia-Cely, Strong gravitational radiation from a simple dark matter model, JHEP 05 (2019) 190 [arXiv:1809.01198] [INSPIRE].

- [81] F.P. Huang and C.S. Li, Probing the baryogenesis and dark matter relaxed in phase transition by gravitational waves and colliders, Phys. Rev. D 96 (2017) 095028 [arXiv:1709.09691] [INSPIRE].
- [82] K. Tsumura, M. Yamada and Y. Yamaguchi, Gravitational wave from dark sector with dark pion, JCAP 07 (2017) 044 [arXiv:1704.00219] [INSPIRE].
- [83] D. Croon, A. Kusenko, A. Mazumdar and G. White, Solitosynthesis and Gravitational Waves, Phys. Rev. D 101 (2020) 085010 [arXiv:1910.09562] [INSPIRE].
- [84] A. Addazi, Y.-F. Cai and A. Marciano, Testing Dark Matter Models with Radio Telescopes in light of Gravitational Wave Astronomy, Phys. Lett. B 782 (2018) 732 [arXiv:1712.03798] [INSPIRE].
- [85] B. Imtiaz, Y.-F. Cai and Y. Wan, Two-field cosmological phase transitions and gravitational waves in the singlet Majoron model, Eur. Phys. J. C 79 (2019) 25 [arXiv:1804.05835] [INSPIRE].
- [86] A. Addazi and A. Marciano, Limiting majoron self-interactions from gravitational wave experiments, Chin. Phys. C 42 (2018) 023105 [arXiv:1705.08346] [INSPIRE].
- [87] Y. Bai, A.J. Long and S. Lu, Dark Quark Nuggets, Phys. Rev. D 99 (2019) 055047
  [arXiv:1810.04360] [INSPIRE].
- [88] L. Bian and X. Liu, Two-step strongly first-order electroweak phase transition modified FIMP dark matter, gravitational wave signals, and the neutrino mass, Phys. Rev. D 99 (2019) 055003 [arXiv:1811.03279] [INSPIRE].
- [89] M. Pandey and A. Paul, Gravitational Wave Emissions from First Order Phase Transitions with Two Component FIMP Dark Matter, arXiv:2003.08828 [INSPIRE].
- [90] H. Davoudiasl, P.B. Denton and J. Gehrlein, Supermassive Black Holes, Ultralight Dark Matter, and Gravitational Waves from a First Order Phase Transition, Phys. Rev. Lett. 128 (2022) 081101 [arXiv:2109.01678] [INSPIRE].
- [91] F.P. Huang and J.-H. Yu, Exploring inert dark matter blind spots with gravitational wave signatures, Phys. Rev. D 98 (2018) 095022 [arXiv:1704.04201] [INSPIRE].
- [92] A. Paul, B. Banerjee and D. Majumdar, Gravitational wave signatures from an extended inert doublet dark matter model, JCAP 10 (2019) 062 [arXiv:1908.00829] [INSPIRE].
- [93] A. Hektor, K. Kannike and V. Vaskonen, Modifying dark matter indirect detection signals by thermal effects at freeze-out, Phys. Rev. D 98 (2018) 015032 [arXiv:1801.06184] [INSPIRE].
- [94] K. Kannike, K. Loos and M. Raidal, Gravitational wave signals of pseudo-Goldstone dark matter in the  $\mathbb{Z}_3$  complex singlet model, Phys. Rev. D 101 (2020) 035001 [arXiv:1907.13136] [INSPIRE].
- [95] K. Kannike and M. Raidal, Phase Transitions and Gravitational Wave Tests of Pseudo-Goldstone Dark Matter in the Softly Broken U(1) Scalar Singlet Model, Phys. Rev. D 99 (2019) 115010 [arXiv:1901.03333] [INSPIRE].
- [96] A. Mohamadnejad, Gravitational waves from scale-invariant vector dark matter model: Probing below the neutrino-floor, Eur. Phys. J. C 80 (2020) 197 [arXiv:1907.08899] [INSPIRE].
- [97] M. Breitbach, J. Kopp, E. Madge, T. Opferkuch and P. Schwaller, Dark, Cold, and Noisy: Constraining Secluded Hidden Sectors with Gravitational Waves, JCAP 07 (2019) 007 [arXiv:1811.11175] [INSPIRE].

- [98] J. Arakawa, A. Rajaraman and T.M.P. Tait, *Annihilogenesis*, *JHEP* **08** (2022) 078 [arXiv:2109.13941] [INSPIRE].
- [99] A. Azatov, M. Vanvlasselaer and W. Yin, Dark Matter production from relativistic bubble walls, JHEP 03 (2021) 288 [arXiv:2101.05721] [INSPIRE].
- [100] A. Azatov and M. Vanvlasselaer, Bubble wall velocity: heavy physics effects, JCAP **01** (2021) 058 [arXiv:2010.02590] [INSPIRE].
- [101] D.J.H. Chung, A.J. Long and L.-T. Wang, 125 GeV Higgs boson and electroweak phase transition model classes, Phys. Rev. D 87 (2013) 023509 [arXiv:1209.1819] [INSPIRE].
- [102] P.S.B. Dev and A. Mazumdar, Probing the Scale of New Physics by Advanced LIGO/VIRGO, Phys. Rev. D 93 (2016) 104001 [arXiv:1602.04203] [INSPIRE].
- [103] R. Jinno, S. Lee, H. Seong and M. Takimoto, Gravitational waves from first-order phase transitions: Towards model separation by bubble nucleation rate, JCAP 11 (2017) 050 [arXiv:1708.01253] [INSPIRE].
- [104] M. Chala, V.V. Khoze, M. Spannowsky and P. Waite, Mapping the shape of the scalar potential with gravitational waves, Int. J. Mod. Phys. A 34 (2019) 1950223 [arXiv:1905.00911] [INSPIRE].
- [105] D. Croon, T.E. Gonzalo, L. Graf, N. Košnik and G. White, GUT Physics in the era of the LHC, Front. in Phys. 7 (2019) 76 [arXiv:1903.04977] [INSPIRE].
- [106] S.A.R. Ellis, S. Ipek and G. White, *Electroweak Baryogenesis from Temperature-Varying Couplings*, *JHEP* **08** (2019) 002 [arXiv:1905.11994] [INSPIRE].
- [107] J. Ellis, M. Lewicki and J.M. No, Gravitational waves from first-order cosmological phase transitions: lifetime of the sound wave source, JCAP 07 (2020) 050 [arXiv:2003.07360] [INSPIRE].
- [108] A. Megevand and F.A. Membiela, Model-independent features of gravitational waves from bubble collisions, Phys. Rev. D 104 (2021) 123532 [arXiv:2108.07034] [INSPIRE].
- [109] K. Schmitz, New Sensitivity Curves for Gravitational-Wave Signals from Cosmological Phase Transitions, JHEP 01 (2021) 097 [arXiv:2002.04615] [INSPIRE].
- [110] T. Alanne, T. Hugle, M. Platscher and K. Schmitz, A fresh look at the gravitational-wave signal from cosmological phase transitions, JHEP 03 (2020) 004 [arXiv:1909.11356] [INSPIRE].
- [111] Y. Bai and M. Korwar, Cosmological constraints on first-order phase transitions, Phys. Rev. D 105 (2022) 095015 [arXiv:2109.14765] [INSPIRE].
- [112] S. Kumar, R. Sundrum and Y. Tsai, Non-Gaussian stochastic gravitational waves from phase transitions, JHEP 11 (2021) 107 [arXiv:2102.05665] [INSPIRE].
- [113] J. Ellis, M. Fairbairn, M. Lewicki, V. Vaskonen and A. Wickens, *Detecting circular polarisation in the stochastic gravitational-wave background from a first-order cosmological phase transition*, *JCAP* **10** (2020) 032 [arXiv:2005.05278] [INSPIRE].
- [114] J.R. Espinosa, T. Konstandin, J.M. No and G. Servant, Energy Budget of Cosmological First-order Phase Transitions, JCAP 06 (2010) 028 [arXiv:1004.4187] [INSPIRE].
- [115] F. Giese, T. Konstandin and J. van de Vis, Model-independent energy budget of cosmological first-order phase transitions A sound argument to go beyond the bag model, JCAP 07 (2020) 057 [arXiv:2004.06995] [INSPIRE].

- [116] F. Giese, T. Konstandin, K. Schmitz and J. van de Vis, Model-independent energy budget for LISA, JCAP 01 (2021) 072 [arXiv:2010.09744] [INSPIRE].
- [117] D. Bödeker and G.D. Moore, Can electroweak bubble walls run away?, JCAP 05 (2009) 009 [arXiv:0903.4099] [INSPIRE].
- [118] D. Bödeker and G.D. Moore, *Electroweak Bubble Wall Speed Limit*, *JCAP* **05** (2017) 025 [arXiv:1703.08215] [INSPIRE].
- [119] S. Höche, J. Kozaczuk, A.J. Long, J. Turner and Y. Wang, Towards an all-orders calculation of the electroweak bubble wall velocity, JCAP 03 (2021) 009 [arXiv:2007.10343] [INSPIRE].
- [120] K. Schmitz, LISA Sensitivity to Gravitational Waves from Sound Waves, Symmetry 12 (2020) 1477 [arXiv:2005.10789] [INSPIRE].
- [121] M. Hindmarsh, S.J. Huber, K. Rummukainen and D.J. Weir, Gravitational waves from the sound of a first order phase transition, Phys. Rev. Lett. 112 (2014) 041301 [arXiv:1304.2433] [INSPIRE].
- [122] M. Hindmarsh, S.J. Huber, K. Rummukainen and D.J. Weir, Numerical simulations of acoustically generated gravitational waves at a first order phase transition, Phys. Rev. D 92 (2015) 123009 [arXiv:1504.03291] [INSPIRE].
- [123] M. Hindmarsh, S.J. Huber, K. Rummukainen and D.J. Weir, Shape of the acoustic gravitational wave power spectrum from a first order phase transition, Phys. Rev. D 96 (2017) 103520 [Erratum ibid. 101 (2020) 089902] [arXiv:1704.05871] [INSPIRE].
- [124] R. Jinno and M. Takimoto, Gravitational waves from bubble dynamics: Beyond the Envelope, JCAP 01 (2019) 060 [arXiv:1707.03111] [INSPIRE].
- [125] D. Cutting, M. Hindmarsh and D.J. Weir, Gravitational waves from vacuum first-order phase transitions: from the envelope to the lattice, Phys. Rev. D 97 (2018) 123513 [arXiv:1802.05712] [INSPIRE].
- [126] D. Cutting, E.G. Escartin, M. Hindmarsh and D.J. Weir, Gravitational waves from vacuum first order phase transitions II: from thin to thick walls, Phys. Rev. D 103 (2021) 023531 [arXiv:2005.13537] [INSPIRE].
- [127] R. Jinno, T. Konstandin and H. Rubira, A hybrid simulation of gravitational wave production in first-order phase transitions, JCAP **04** (2021) 014 [arXiv:2010.00971] [INSPIRE].
- [128] J. Dahl, M. Hindmarsh, K. Rummukainen and D. Weir, Decay of acoustic turbulence in two dimensions and implications for cosmological gravitational waves, arXiv:2112.12013 [INSPIRE].
- [129] P. Auclair et al., Generation of gravitational waves from freely decaying turbulence, arXiv:2205.02588 [INSPIRE].
- [130] M. Quirós, Finite temperature field theory and phase transitions, in ICTP Summer School in High-Energy Physics and Cosmology, Trieste, Italy, June 29–July 17, 1998, pp. 187–259 [hep-ph/9901312] [INSPIRE].
- [131] C.L. Wainwright, CosmoTransitions: Computing Cosmological Phase Transition Temperatures and Bubble Profiles with Multiple Fields, Comput. Phys. Commun. 183 (2012) 2006 [arXiv:1109.4189] [INSPIRE].
- [132] M.J. Ramsey-Musolf, The electroweak phase transition: a collider target, JHEP **09** (2020) 179 [arXiv:1912.07189] [INSPIRE].

- [133] S. Akula, C. Balázs and G.A. White, Semi-analytic techniques for calculating bubble wall profiles, Eur. Phys. J. C 76 (2016) 681 [arXiv:1608.00008] [INSPIRE].
- [134] M. Dine, R.G. Leigh, P.Y. Huet, A.D. Linde and D.A. Linde, Towards the theory of the electroweak phase transition, Phys. Rev. D 46 (1992) 550 [hep-ph/9203203] [INSPIRE].
- [135] H.-K. Guo, K. Sinha, D. Vagie and G. White, *Phase Transitions in an Expanding Universe: Stochastic Gravitational Waves in Standard and Non-Standard Histories*, *JCAP* **01** (2021) 001 [arXiv:2007.08537] [INSPIRE].
- [136] A. Kosowsky and M.S. Turner, Gravitational radiation from colliding vacuum bubbles: envelope approximation to many bubble collisions, Phys. Rev. D 47 (1993) 4372 [astro-ph/9211004] [INSPIRE].
- [137] M. Lewicki and V. Vaskonen, On bubble collisions in strongly supercooled phase transitions, Phys. Dark Univ. 30 (2020) 100672 [arXiv:1912.00997] [INSPIRE].
- [138] M. Hindmarsh, Sound shell model for acoustic gravitational wave production at a first-order phase transition in the early Universe, Phys. Rev. Lett. 120 (2018) 071301 [arXiv:1608.04735] [INSPIRE].
- [139] H.-K. Guo, K. Sinha, D. Vagie and G. White, The benefits of diligence: how precise are predicted gravitational wave spectra in models with phase transitions?, JHEP 06 (2021) 164 [arXiv:2103.06933] [INSPIRE].
- [140] C.-W. Chiang and E. Senaha, On gauge dependence of gravitational waves from a first-order phase transition in classical scale-invariant U(1)' models, Phys. Lett. B 774 (2017) 489 [arXiv:1707.06765] [INSPIRE].
- [141] L. Niemi, P. Schicho and T.V.I. Tenkanen, Singlet-assisted electroweak phase transition at two loops, Phys. Rev. D 103 (2021) 115035 [arXiv:2103.07467] [INSPIRE].
- [142] R.-G. Cai, M. Sasaki and S.-J. Wang, The gravitational waves from the first-order phase transition with a dimension-six operator, JCAP 08 (2017) 004 [arXiv:1707.03001] [INSPIRE].
- [143] M. Chala, C. Krause and G. Nardini, Signals of the electroweak phase transition at colliders and gravitational wave observatories, JHEP 07 (2018) 062 [arXiv:1802.02168] [INSPIRE].
- [144] O. Gould and J. Hirvonen, Effective field theory approach to thermal bubble nucleation, Phys. Rev. D 104 (2021) 096015 [arXiv:2108.04377] [INSPIRE].
- [145] O. Gould and T.V.I. Tenkanen, On the perturbative expansion at high temperature and implications for cosmological phase transitions, JHEP 06 (2021) 069 [arXiv:2104.04399] [INSPIRE].
- [146] P.M. Schicho, T.V.I. Tenkanen and J. Österman, Robust approach to thermal resummation: Standard Model meets a singlet, JHEP 06 (2021) 130 [arXiv:2102.11145] [INSPIRE].
- [147] O. Gould, Real scalar phase transitions: a nonperturbative analysis, JHEP **04** (2021) 057 [arXiv:2101.05528] [INSPIRE].
- [148] M. Postma and G. White, Cosmological phase transitions: is effective field theory just a toy?, JHEP 03 (2021) 280 [arXiv:2012.03953] [INSPIRE].
- [149] D. Cutting, M. Hindmarsh and D.J. Weir, Vorticity, kinetic energy, and suppressed gravitational wave production in strong first order phase transitions, Phys. Rev. Lett. 125 (2020) 021302 [arXiv:1906.00480] [INSPIRE].

- [150] A. Roper Pol, S. Mandal, A. Brandenburg, T. Kahniashvili and A. Kosowsky, Numerical simulations of gravitational waves from early-universe turbulence, Phys. Rev. D 102 (2020) 083512 [arXiv:1903.08585] [INSPIRE].
- [151] Lattice Strong Dynamics collaboration, Stealth dark matter confinement transition and gravitational waves, Phys. Rev. D 103 (2021) 014505 [arXiv:2006.16429] [INSPIRE].
- [152] M. Lewicki and V. Vaskonen, Gravitational waves from colliding vacuum bubbles in gauge theories, Eur. Phys. J. C 81 (2021) 437 [Erratum ibid. 81 (2021) 1077] [arXiv:2012.07826] [INSPIRE].
- [153] D. Cutting, Simulations of early universe phase transitions and gravitational waves, Ph.D. Thesis, University of Sussex, Broghton, U.K. (2021).
- [154] R. Jinno, T. Konstandin, H. Rubira and J. van de Vis, Effect of density fluctuations on gravitational wave production in first-order phase transitions, JCAP 12 (2021) 019 [arXiv:2108.11947] [INSPIRE].
- [155] P. Schicho, T.V.I. Tenkanen and G. White, Combining thermal resummation and gauge invariance for electroweak phase transition, arXiv:2203.04284 [INSPIRE].
- [156] R. van Haasteren et al., Placing limits on the stochastic gravitational-wave background using European Pulsar Timing Array data, Mon. Not. Roy. Astron. Soc. 414 (2011) 3117 [Erratum ibid. 425 (2012) 1597] [arXiv:1103.0576] [INSPIRE].
- [157] NANOGRAV collaboration, The NANOGRAV 12.5 yr Data Set: Search for an Isotropic Stochastic Gravitational-wave Background, Astrophys. J. Lett. 905 (2020) L34 [arXiv:2009.04496] [INSPIRE].
- [158] T.J.W. Lazio et al., Solar System Ephemerides, Pulsar Timing, Gravitational Waves, & Navigation, IAU Symp. 337 (2017) 150 [arXiv:1801.02898] [INSPIRE].
- [159] Gaia collaboration, *Gaia Data Release 2*: Summary of the contents and survey properties, *Astron. Astrophys.* **616** (2018) A1 [arXiv:1804.09365] [INSPIRE].
- [160] G. Janssen et al., Gravitational wave astronomy with the SKA, PoS AASKA14 (2015) 037 [arXiv:1501.00127] [INSPIRE].
- [161] A. Vallenari, The future of astrometry in space, Front. Astron. Space Sci.s 5 (2018) 1.
- [162] LISA collaboration, Laser Interferometer Space Antenna, arXiv:1702.00786 [INSPIRE].
- [163] T. Robson, N.J. Cornish and C. Liu, The construction and use of LISA sensitivity curves, Class. Quant. Grav. 36 (2019) 105011 [arXiv:1803.01944] [INSPIRE].
- [164] W.-H. Ruan, Z.-K. Guo, R.-G. Cai and Y.-Z. Zhang, *Taiji program: Gravitational-wave sources*, *Int. J. Mod. Phys. A* **35** (2020) 2050075 [arXiv:1807.09495] [INSPIRE].
- [165] TianQin collaboration, *TianQin: a space-borne gravitational wave detector*, *Class. Quant. Grav.* **33** (2016) 035010 [arXiv:1512.02076] [INSPIRE].
- [166] X. Gong et al., Descope of the ALIA mission, J. Phys. Conf. Ser. 610 (2015) 012011 [arXiv:1410.7296] [INSPIRE].
- [167] V. Corbin and N.J. Cornish, Detecting the cosmic gravitational wave background with the big bang observer, Class. Quant. Grav. 23 (2006) 2435 [gr-qc/0512039] [INSPIRE].
- [168] K. Yagi and N. Seto, Detector configuration of DECIGO/BBO and identification of cosmological neutron-star binaries, Phys. Rev. D 83 (2011) 044011 [Erratum ibid. 95 (2017) 109901] [arXiv:1101.3940] [INSPIRE].

- [169] S. Kawamura et al., Current status of space gravitational wave antenna DECIGO and B-DECIGO, PTEP 2021 (2021) 05A105 [arXiv:2006.13545] [INSPIRE].
- [170] S. Kawamura et al., The Japanese space gravitational wave antenna DECIGO, Class. Quant. Grav. 23 (2006) S125 [INSPIRE].
- [171] LIGO Scientific collaboration, Gravitational wave astronomy with LIGO and similar detectors in the next decade, arXiv:1904.03187 [INSPIRE].
- [172] LIGO SCIENTIFIC collaboration, Advanced LIGO, Class. Quant. Grav. 32 (2015) 074001 [arXiv:1411.4547] [INSPIRE].
- [173] T.L.S. Collaboration, LIGO DCC-T1400316, technical notes (2014).
- [174] M. Punturo et al., The Einstein Telescope: A third-generation gravitational wave observatory, Class. Quant. Grav. 27 (2010) 194002 [INSPIRE].
- [175] LIGO Scientific collaboration, Exploring the Sensitivity of Next Generation Gravitational Wave Detectors, Class. Quant. Grav. 34 (2017) 044001 [arXiv:1607.08697] [INSPIRE].
- [176] A. Sesana et al., Unveiling the gravitational universe at  $\mu$ -Hz frequencies, Exper. Astron. 51 (2021) 1333 [arXiv:1908.11391] [INSPIRE].
- [177] A. Kobakhidze, C. Lagger, A. Manning and J. Yue, Gravitational waves from a supercooled electroweak phase transition and their detection with pulsar timing arrays, Eur. Phys. J. C 77 (2017) 570 [arXiv:1703.06552] [INSPIRE].
- [178] J. Ellis, M. Lewicki, J.M. No and V. Vaskonen, Gravitational wave energy budget in strongly supercooled phase transitions, JCAP **06** (2019) 024 [arXiv:1903.09642] [INSPIRE].
- [179] J. Ellis, M. Lewicki and V. Vaskonen, Updated predictions for gravitational waves produced in a strongly supercooled phase transition, JCAP 11 (2020) 020 [arXiv:2007.15586] [INSPIRE].
- [180] X. Wang, F.P. Huang and X. Zhang, Phase transition dynamics and gravitational wave spectra of strong first-order phase transition in supercooled universe, JCAP **05** (2020) 045 [arXiv:2003.08892] [INSPIRE].
- [181] D. Croon, O. Gould, P. Schicho, T.V.I. Tenkanen and G. White, Theoretical uncertainties for cosmological first-order phase transitions, JHEP 04 (2021) 055 [arXiv:2009.10080] [INSPIRE].